Final Report – Supplemental Research

DETERMINE OPTIMUM DEPTHS OF DRILLED SHAFTS SUBJECTEDTO COMBINED TORSION AND LATERAL LOADS FROM CENTRIFUGE TESTING (USING KB POLYMER SLURRY)

UF Project No.: 4910-4554-015-12

Contract No.: BD-545, WO #4

Submitted to:

Florida Department of Transportation
605 Suwannee Street, MS 30
Tallahassee, FL 32399-0450

UNIVERSITY OF FLORIDA

Michael McVay
Zhihong Hu
Department of Civil and Coastal Engineering
College of Engineering
365 Weil Hall, P.O. Box 116580
Gainesville, FL 32611-6580
Tel: (352) 392-8697 SunCom: 622-8697
Fax: (352) 392-3394

October 2003

Technical Report Documentation Page

1. Report No.: Final Report Supplemental Research

2. Government Accession No.:

3. Recipient's Catalog No.:

4. Title and Subtitle: Determine Optimum Depths of Drilled Shafts Subjected to Combined Torsion and Lateral Loads from Centrifuge Testing (Using KB Polymer Slurry) – Supplemental Research

5. Report Date: October 2003

6. Performing Organization Code:

7. Author(s): Dr. Michael C. McVay and Zhihong Hu

8. Performing Organization Report No.: 4910-4554-015-12

9. Performing Organization Name and Address:
University of Florida
Department of Civil and Coastal Engineering
365 Weil Hall / P.O. Box 116580
Gainesville, FL 32611-6580

10. Work Unit No. (TRAIS):

11. Contract or Grant No.: BD-545, WO #4

12. Sponsoring Agency Name and Address:
Florida Department of Transportation
Research Management Center
605 Suwannee Street, MS 30
Tallahassee, FL 32301-8064

13. Type of Report and Period Covered: Final Rep.–Supplemental Research; April 25, 2003 – September 30, 2003

14. Sponsoring Agency Code:

15. Supplementary Notes:

Prepared in cooperation with the Federal Highway Administration

16. Abstract

Sixteen centrifuge tests were conducted on high mast sign/signal structures (mast arm, pole, drilled shaft). The foundations, drilled shafts (25′ and 25′ embedment), were constructed in saturated sands under two different soil densities (loose and dense) using polymer slurry in their construction. The shafts were constructed with cement grout, steel reinforcement and spun in the centrifuge while still fluid, allowing the soil stresses around the shafts to equilibrate to field (prototype) values. The sign/signal structures were laterally loaded at three different points: 1) pole; 2) mid mast arm; and 3) mast arm tip. Loading on the pole applied no torque to the foundation, whereas loading on the mast arm and arm tip applied increasing values of torque.

All of the lateral load tests with torque (i.e., mid mast and arm tip) failed through foundation rotation (failure: 15°). The latter is attributed to the reduced vertical and horizontal effective stresses in the saturated vs. dry sands. The torsional resistance was found independent of lateral load magnitude, as well as soil properties (i.e., sand density, strength, etc.). However, the lateral resistance of the shafts was found significantly affected by the applied torque on the foundation. The reduction in lateral resistance as a function of torque to lateral load ratio graphs developed in FDOT project BC354, RPWO #9 predicted quite satisfactorily the shafts lateral response.

For the polymer slurry shaft construction, it was noted that no cake formation occurred. However, the torsional resistance of the shafts, especially in dense sands was higher than the mineral bentonite slurry. The latter was attributed to the polymer slurry penetrating within the borehole wall and bonding with shaft, as well as reinforcing the soil.

Finally, the Mathcad file (FDOT project BC354, RPWO #9) developed to design/analyze high mast sign/signal pole structures for both lateral and torsional loading predicted the experiments satisfactorily.

17. Key Words:
Drilled shaft
Torque and lateral loading
Centrifuge testing
Saturated sands
Polymer slurry construction

18. Distribution Statement:
No restrictions. This document is available to the public through the National Technical Information Service, Springfield, VA, 22161

19. Security Classif. (of this report): Unclassified

20. Security Classif. (of this page): Unclassified

21. No. of Pages: 44

22. Price:

Form DOT F 1700.7 (8-72)

DISCLAIMER

SI* (MODERN METRIC) CONVERSION FACTORS

APPROXIMATE CONVERSIONS TO SI UNITS

Symbol	When You Know	Multiply By	To Find	Symbol
		LENGTH		
in	inches	25.4	millimeters	mm
ft	feet	0.305	meters	m
yd	yards	0.914	meters	m
mi	miles	1.61	kilometers	km
		AREA		
in^2	square inches	645.2	square millimeters	mm^2
ft^2	square feet	0.093	square meters	m^2
yd^2	square yards	0.836	square meters	m^2
ac	acres	0.405	hectares	ha
mi^2	square miles	2.59	square kilometers	km^2
		VOLUME		
fl oz	fluid ounces	29.57	milliliters	ml
gal	gallons	3.785	liters	l
ft^3	cubic feet	0.028	cubic meters	m^3
yd^3	cubic yards	0.765	cubic meters	m^3

NOTE: Volumes greater than 1000 l shall be shown in m^3.

Symbol	When You Know	Multiply By	To Find	Symbol
		MASS		
oz	ounces	28.35	grams	g
lb	pounds	0.454	kilograms	kg
T	short tons (2000 lb)	0.907	megagrams	Mg
		TEMPERATURE (exact)		
°F	Fahrenheit temperature	5(F-32)/9 or (F-32)/1.8	Celcius temperature	°C
		ILLUMINATION		
fc	foot-candles	10.76	lux	l
fl	foot-Lamberts	3.426	candela/m^2	cd/m^2
		FORCE and PRESSURE or STRESS		
lbf	poundforce	4.45	newtons	N
psi	poundforce per square inch	6.89	kilopascals	kPa

APPROXIMATE CONVERSIONS FROM SI UNITS

Symbol	When You Know	Multiply By	To Find	Symbol
		LENGTH		
mm	millimeters	0.039	inches	in
m	meters	3.28	feet	ft
m	meters	1.09	yards	yd
km	kilometers	0.621	miles	mi
		AREA		
mm^2	square millimeters	0.0016	square inches	in^2
m^2	square meters	10.764	square feet	ft^2
m^2	square meters	1.195	square yards	yd^2
ha	hectares	2.47	acres	ac
km^2	square kilometers	0.386	square miles	mi^2
		VOLUME		
ml	milliliters	0.034	fluid ounces	fl oz
l	liters	0.264	gallons	gal
m^3	cubic meters	35.71	cubic feet	ft^3
m^3	cubic meters	1.307	cubic yards	yd^3
		MASS		
g	grams	0.035	ounces	oz
kg	kilograms	2.202	pounds	lb
Mg	megagrams	1.103	short tons (2000 lb)	T
		TEMPERATURE (exact)		
°C	Celcius temperature	1.8C + 32	Fahrenheit temperature	°F
		ILLUMINATION		
lx	lux	0.0929	foot-candles	fc
cd/m^2	candela/m^2	0.2919	foot-Lamberts	fl
		FORCE and PRESSURE or STRESS		
N	newtons	0.225	poundforce	lbf
kPa	kilopascals	0.145	poundforce per square inch	psi

* SI is the symbol for the International System of Units. Appropriate rounding should be made to comply with Section 4 of ASTM E380.

(Revised August 1992)

TABLE OF CONTENTS

LIST OF TABLES

LIST OF FIGURES

CHAPTER 1
INTRODUCTION

1.1 Background

Prior research (FDOT project: BC354, RPWO #9) focused on the behavior of drilled shafts subject to combined lateral and torsional loading. More than eighty centrifuge tests were conducted on sign/signal mast arms supported on drilled shafts founded in sand. Three different length to diameter ratios, and three different loadings (on pole, middle of mast arm, and mast arm tip), were performed in both dry and saturated sands. The shaft construction considered both steel casing and bentonite slurry.

The tests revealed a strong coupling between lateral shaft resistance and applied torque. Specifically, anywhere from 10% to 50% reduction in lateral shaft resistance occurs with torque. Also, in the case of construction with bentonite slurry, wall cake thickness of 0.5 inch or less had a negligible influence on the shaft’s torsional resistance. However construction, which resulted in bentonite cake thickness of 2.0 inches or more, resulted in 50% reduction in torsional resistance.

Since drilled shaft foundation construction for sign/signal system allows for the use of polymer (synthetic) slurry for wall stabilization, it was decided to repeat a number of the experiments for polymers. This report focuses on the torsional lateral resistance of drilled shafts constructed with KB polymer.

1.2 Synthetic Polymer Slurries

Polymer slurries used in drilled shaft construction are composed of unit cells or monomers linked together in either straight or branched chains to form macromolecules. In general, the repeating units or monomers, when combined in pairs or more, form copolymers.

The first synthetic slurry materials were introduced approximately thirty years ago. They were made from Carboxymethylcellulose (CMC), which is derived from wood pulp, Guar and Xanthan. Some typical problems with these slurries were high rates of fluid loss causing excavation instability; concrete-slurry compatibility; rebar bonding and loss of concrete compressive strength. At that time they were considered unacceptable for replacement of bentonite slurry.

In the mid-1980's, the first truly synthetic polymers began to make their way into the geo-construction industry. The first of these products was a long chain anionic PHPA used in oil drilling. PHPAs are high molecular weight, long chain, synthetic polymers containing numerous negatively charged sites distributed across their backbone, or their threadlike strand. PHPA polymers, as with most types of polymers and bentonite require that a certain minimum concentration of material is maintained in the slurry, or water will grab onto these soil sites and swelling will begin. Sloughing and caving of the walls as well as equalization of pore water pressures follow soil swelling. Therefore, PHPAs have in no way replaced the need for bentonite as the base constituent of an oil and gas drilling fluid. Due to the singular negative charge of the PHPA, they have not proven effective at preventing fluid loss into a porous formation. The development of real differential pressure from the fluid against the formation is also not possible with a PHPA system, because the absence of a cake or membrane.

Consequently, KB Technologies' developed in the early 1990's slurry SlurryPro Vinyl System specifically for earth stabilization. The slurry is made from vinyl polymer strands which are long chain molecules carrying multiple negative and positive charged sites on the polymer stand's surface. One of slurry's most innovative and important improvements is its ability to form an instantaneous soft chemical grout within the exposed sidewall of the excavation. Also, the vinyl polymer strands have numerous arms extending out from each strand that are hydrophobic, which means not water-soluble. These hydrophobic arms look for other hydrophobic arms extending from other vinyl polymer strands, joining these polymer strands together in an organized inter-linked or three dimensional net, or web like system. This associative characteristic in combination with the dual charge nature of the vinyl slurry system allows the polymer to bond, or lock, on to any type of soil surface with ease causing it to create a unique semi-plastic membrane, or barrier, at and within the soil interface, which is useful for the controlling fluid loss. Of interest for this work was the influence of the slurry on the shaft's capacity.

CHAPTER 2
CENTRIFUGE TESTS

2.1 Prototype/Centrifuge Model

Typical sign/signal/lighting poles vary in height from 5.5 m to 8.5 m; have mast arm lengths ranging from 4.5 m to 15 m, and shaft diameters varying from 1 m to 2 m with embedment ranging from 3 m to 12 m. Since the focus of this study was the influence of torque on the lateral resistance of shafts for different L/D (length to diameter ratio) ratios and soil strengths, it was decided to select one pole height (6.1 m), and one shaft diameter (1.52 m). The loading was applied as a point load at one of three locations: 0 m (on the pole), 4.25 m and 6 m along the mast arm.

It is generally recognized (Reese, 1988) that the construction process impacts the axial and lateral resistance of a drilled shaft by modifying the insitu stresses. To replicate the field construction process, it was decided to place the reinforcing cage, pole, and mast arm in fluid cement grout while the centrifuge was stopped (Figure 2.1), spin the experiment up to 45 g's, allow the cement grout time to set, and then run the lateral load/torsion test. Spinning the experiment while the grout was still fluid, as well as not stopping the experiment until the torque/lateral load testing had been finished, ensured that the soil and shaft stresses were at field (prototype) values.

The sign/signal/lighting pole was modeled with a steel pipe (OD: 21.25mm, ID: 17 mm). To ensure fixity between the mast arm/pole and drilled shaft, and provide reinforcement for the drilled shaft, the pole was extended into the shaft as longitudinal steel reinforcement (resists bending moment). The steel area ratio, ρ (seven percent), was obtained by milling ten slots into the pipe below ground surface. A 1/N scaling (Bradley, 1984) relationship (N: centrifuge acceleration) was used to size both the model steel reinforcement and shaft dimensions (i.e., diameter & length) with the field.

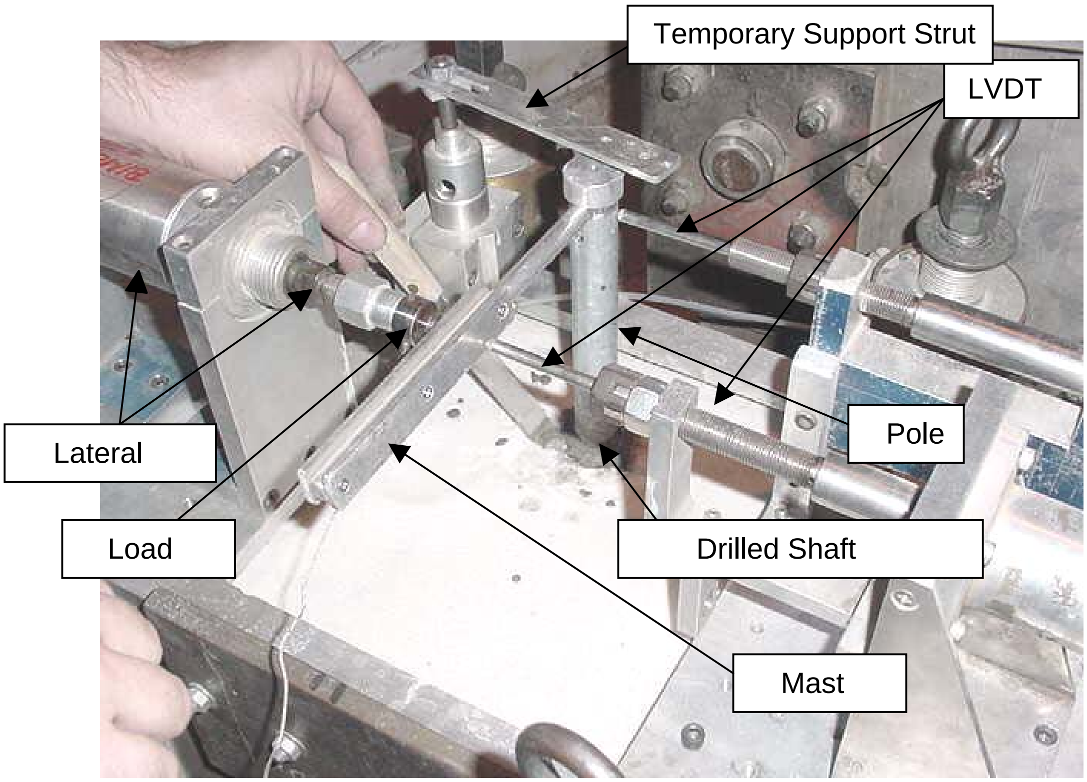

Figure 2.1 Shaft, Pole, Mast Arm, Load and Measuring System

Similar to the field, shear steel was wrapped around the slotted steel longitudinal reinforcement. Figure 2.2 shows a drilled shaft, pole and mast arm, after a lateral load/torque test was completed. Figure 2.3, shows a close-up of the cement grout, and exposed longitudinal, and spiral steel reinforcement. Note, the exposure of the steel reinforcement occurred only after striking the shaft multiple times with a hammer.

The shaft reinforcement, pole and mast arm were supported while the cement grout was fluid with the support strut shown in Figure 2.2. After hydration of the cement grout

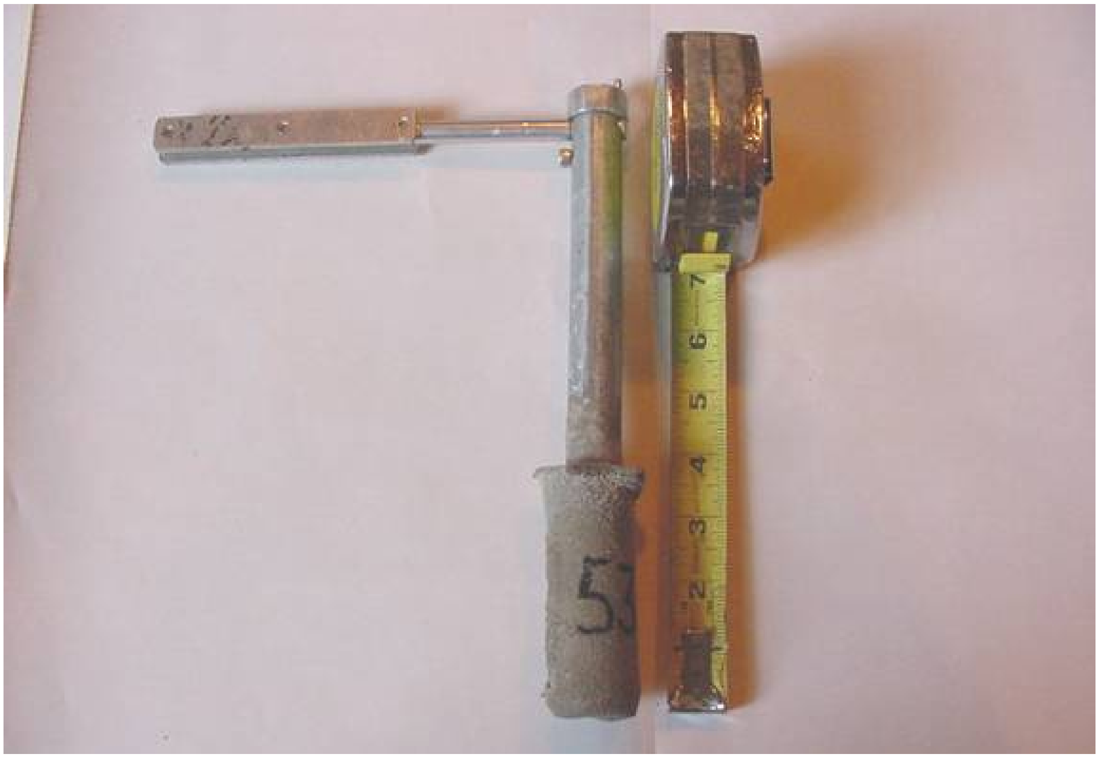

Figure 2.2 Model of Typical Structure and Foundation (L/D = 5)

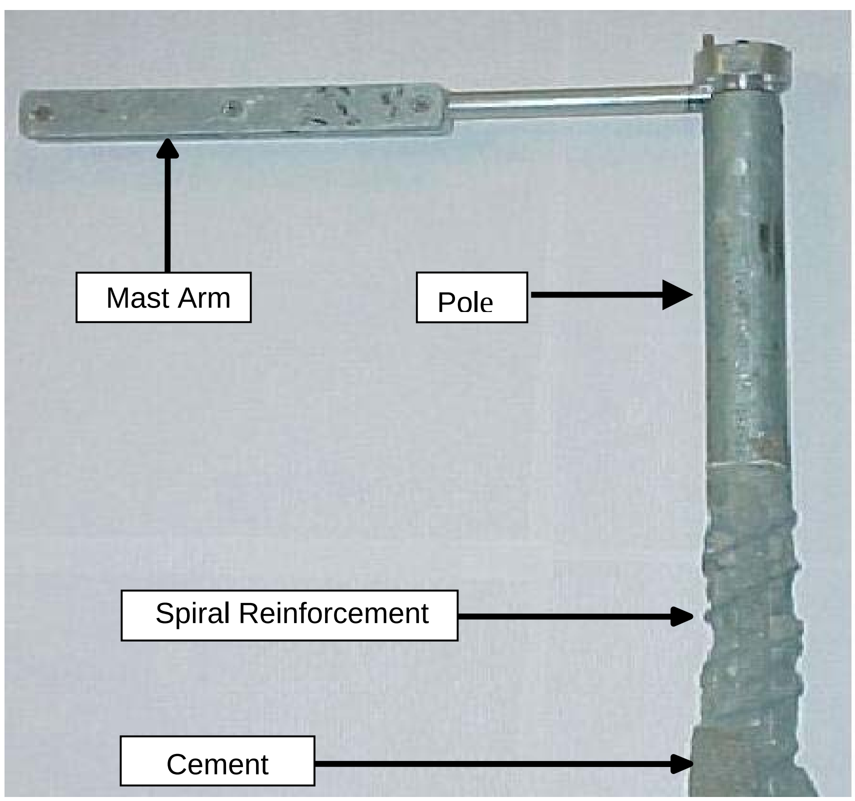

Figure 2.3 Vertical and Spiral Reinforcement in Drilled Shaft

(i.e., drilled shaft), the strut was removed (lifted up) with the vertical air piston while the centrifuge was spinning (approximately five hours after spinning began) and the lateral/torque test performed. To accelerate the cement grout hydration, high early strength cement, plasticizers (improved workability), and accelerators were employed.

To measure deformations, three LVDTs were employed as shown in Figure 2.2. The LVDTs at the top and bottom of the pole measured both lateral movement and rotation of the pole. The LVDT at point of load application on the mast arm and at the top of pole measured both lateral movement and rotation of the mast arm. During the tests, real time plots of load vs. displacements and rotations were monitored until failure was obtained.

In general two types of failure are possible with a sign/signal/lighting system. The first is excessive lateral deflection of the top of the sign/signal/lighting pole, which may result in the mast arm rotating downward, and contacting a passing vehicle (i.e., semi-trucks). The second mode of failure involves rotation of the foundation and the superstructure, i.e., mast arm. In the case of significant rotations, the motorists may have difficulty interpreting the sign, which may become a hazard to both vehicles and pedestrians. For this study, the following FDOT failure was used: 1) lateral movement of 300 mm (6.7 mm model) at the top of a foundation and 2) foundation rotation of fifteen degrees or more.

2.2 Test Sand

The soil used in this study was fine silica-quartz sand (e_{max} =0.85, and e_{min} = 0.58), obtained from Edgar, Florida. Figure 2.4 shows three different grain size curves resulting in the Unified Soil classification of SP. In the centrifuge, the soil scales (45 g's) as a sandy gravel.

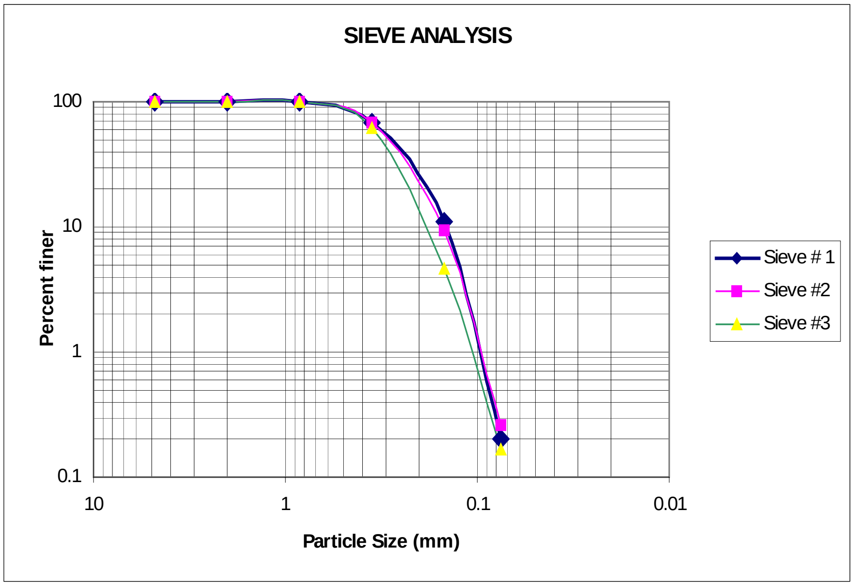

Figure 2.4 Sieve Analysis of Edgar Sand

As with any sand, strength and stiffness is controlled by its relative density or unit weight and moisture content. Of significant importance were the available sand unit weights and relative densities in the experimental container obtained by raining. McVay et al. (1999) showed raining the sand through sieves, located above the centrifuge bucket, resulted in both uniform and reproducible specimens (void ratio and relative densities). After sufficient testing, drop heights (distance from bottom of the sieve to top of container) of 0.5m, 0.85m, and 1.15m were selected. The latter drop heights resulted in sample relative densities, D_r, of 29, 50.7 and 63.5 percent, respectively. Corresponding, angles of internal friction, ϕ, of 32.5, 34.5 and 37 degrees were obtained from direct shear tests on the dry sand.

2.3 Test Procedure

The first step in the test procedure was to prepare the saturated sand to one of the specified densities. Next, a hole was excavated to the correct depth through the use of a casing. Then, the water in the hole was displaced with slurry and the casing was removed. Next, the sample was spun in the centrifuge to simulate the field stresses. Then, the cement grout was tremied into the hole displacing the slurry, the model shaft was inserted into the cement grout and the experiment was spun in the centrifuge to 45g. After 5 hours (cement hydrates), a force was applied to the model. A data acquisition system was used to measure the force and displacement recorded. A discussion of each process follows.

2.3.1 Saturated Sand Preparation

In order to ensure that the sand remained saturated over the history of the test, a sealed Plexiglas tank was installed in the centrifuge bucket, and two plastic garbage bags were placed inside the tank (prevent damage). Next, the dry sand was rained into the centrifuge container through a sieve with 1/16-in. square mesh, Figure 2.5. After sand

Figure 2.5 Raining Sand in Centrifuge Container

placement, two plastic flexible tubes were attached on the sides in the container from the top to the bottom, Figure 2.6. Then water was allowed to flow from a bucket, Figure 2.6, into the soil from the bottom upward, generating minimum air entrainment and soil disturbance. For loose sand (Dr = 34%), the outlined approach generated a unit weight, 92.8 pcf (dry).

Figure 2.6 Saturating the Sand Deposit

In the case of the dense sand deposit (Dr =69%), a vibrating table was employed. The process involved raining the dry sand, filling the container with water, and then vibrating the whole container with sand, and water on the table (Figure 2.7). A dry unit weight of 99.2 pcf was obtained with this procedure.

2.3.2 Polymer Slurry Placement

After raining the saturated sand, a plastic cover was placed on the top of soil (prevent evaporation), and the aluminum-loading frame, Figure 2.8, was attached to the top of the centrifuge container. Next, a wooden plate with a hole for the casing to pass through was

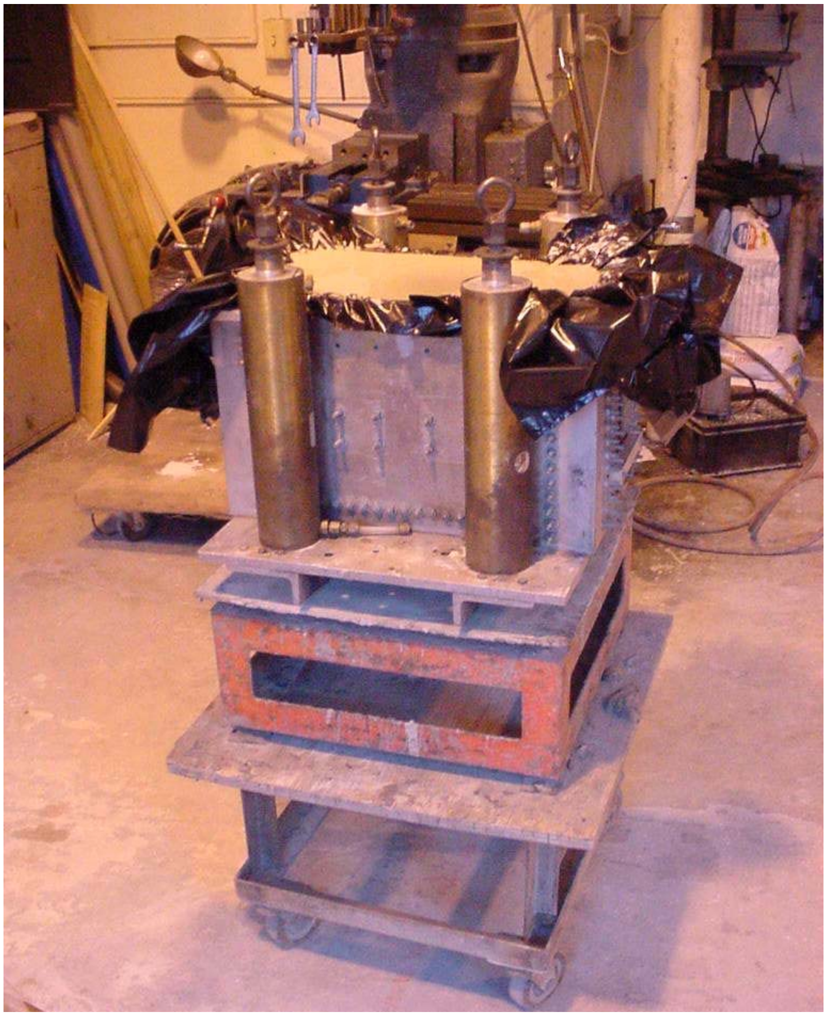

Figure 2.7 Vibrating Saturated Sand Deposit for Dr = 69%

Figure 2.8 Container with the Aluminum Plate

attached to the top-loading frame, Figure 2.8. Subsequently, the centrifuge bucket and loading frame was placed in the centrifuge by lift. In the centrifuge, a plastic tube was pushed into the saturated sand through the wood plate. Next, the sand within the tube was dug out with a spoon, ensuring that the water level in the tube was kept higher than the ground level. Subsequently, the slurry was poured into the tube from the bottom to displace the water. Then the tube was pulled up slowly to allow the slurry to make contact with the sand. Figures 2.9 and 2.10 show the latter process.

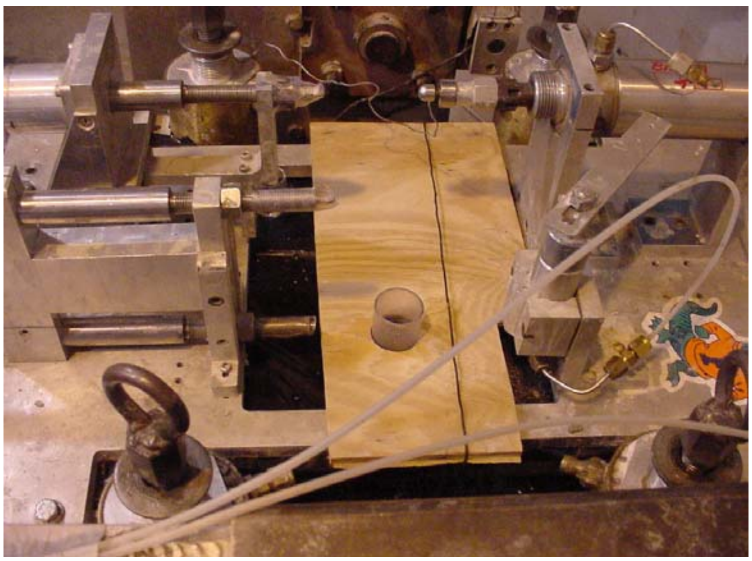

Figure 2.9 Inserting the Tube into the Saturated Sand

Figure 2.10 Pouring Slurry to Displace the Water

2.3.3 Hole Excavation Stability

As identified earlier, the first stage of this research (FDOT project: BC354, RPWO #9) employed bentonite slurry. Bentonite slurry was found to form a slurry cake on the walls of the hole, which greatly diminished the required slurry volume. For instance, the tube that was used to make the hole was pulled up and 4 in. of slurry (i.e., above ground surface) was maintained. For the latter, the centrifuge was spun to 10 g's for 30 seconds, stopped, and the slurry was refilled to 4 in. Next, the bucket was spun to 20 g acceleration for 1 min, and the centrifuge was stopped and the slurry was refilled again. Finally, the bucket was spun to 45 g's for 15 minutes, and stopped. The first two steps were used to form the slurry cake for the following 15 minutes in 45 g. After 15 minutes of spinning, the slurry head dropped to 1 in., which equaled 45 in. or about 4 ft in the prototype.

In the case of polymer slurry, KB SlurryPro CDP (Vinyl), it was found that the slurry head loss was much greater than with the bentonite. Moreover, the volume of the slurry in the plastic tube (Fig. 2.10) was insufficient for the losses during acceleration. Specifically, the slurry head dropped too close to the water level, and the hole began to collapse. In order to provide enough polymer slurry for the expected losses, a large rectangular tank, Figure 2.11, was installed on the centrifuge arm. Attached to the tank was a flexible tube, which was routed to the plastic pipe (Fig. 2.11), sticking out of the saturated ground. Because the slurry head in the tank was higher than that of the plastic pipe, the slurry flowed from the tank through the tube continuously. Consequently, the head in the tube was kept 2 to 3 inches above the ground line during the spinning, stabilizing the hole.

Because there was no slurry cake formed along the wall of the hole, the polymer slurry entered the soil faster than the bentonite slurry. It was found that after a couple of

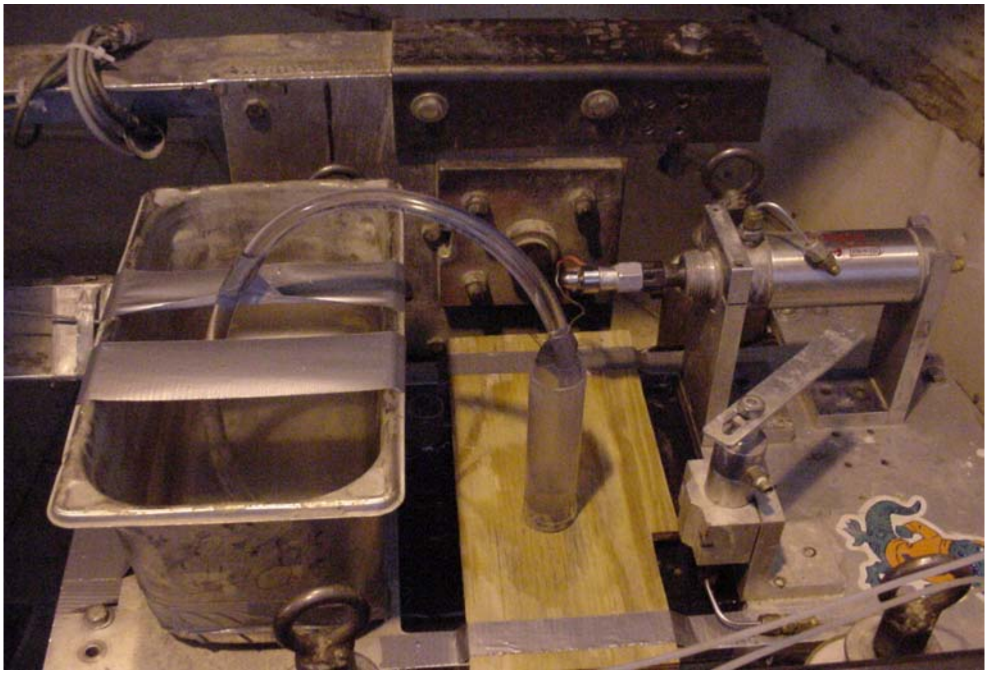

Figure 2.11 Equipment Used for Polymer Slurry

minutes of spinning in 45 g, the polymer slurry had already entered the soil to a distance of twice the diameter. Therefore, it was not necessary to spin the slurry for a longer amount of time. The head in the tank was kept at 3 in before spinning. After 30 seconds of spinning, the centrifuge was stopped, and more slurry was added into the tank to keep a 3 in head. Then after another 30 seconds of spinning was finished, the tank was refilled again and the centrifuge was spun for 1 more minute, and stopped. Careful inspection of the hole showed no cake formation, as well as a steady consumption of slurry during excavation.

2.3.4 Construction of a Drilled Shaft

In order to displace the slurry, the cement grout must be tremied into the hole from the bottom, and must have enough head to push the slurry out. To accomplish the latter, the following process was employed. First the cement grout was squeezed into a long plastic tube as shown in Figure 2.12. Next the tremie pipe had a rubber plug inserted in the top of

Figure 2.12 Placing Cement Grout in Tremie Pipe

the tube, and tape was placed on the bottom of the tube. Subsequently, the tube was inserted to the bottom of the slurry filled hole, and the rubber plug was removed, allowing the cement grout to flow out of the tube displacing the slurry. Figure 2.13 shows the slurry displacement during the cement grouting process.

2.3.5 Construction of the Sign/Pole System

After the cement grout placement, Fig. 2.13, the model (sign pole, mast arm, etc.) was inserted into the shaft. The most important step during this process was to ensure the model rebar cage (shaft reinforcement) was centered in the cement grout and at the correct depth. To assist with the placement a jig was employed which both centered and assessed the cage's elevation. Figure 2.14 shows the placement of the sign pole and reinforcing cage in the cement grout.

After placement of sign pole, the arm was put on the top of the model, and any extra slurry and concrete were removed from around the pole. The arm connected to the small air piston (Fig. 2.14), located at top of the model, to stabilize the structure during centrifuge spinning while the cement grout was still fluid.   Next, the centrifuge was spunup to 176 rpm,

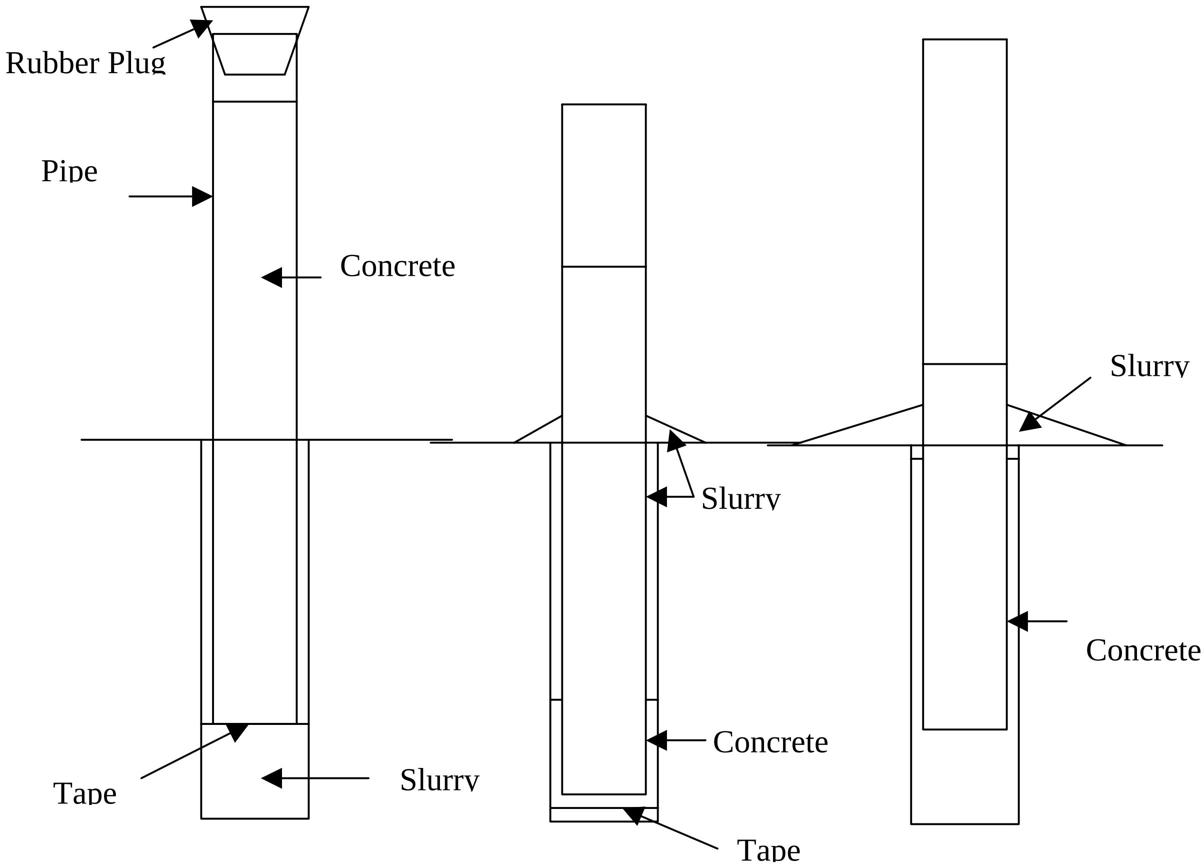

Figure 2.13 Process of Pouring Concrete into the Hole

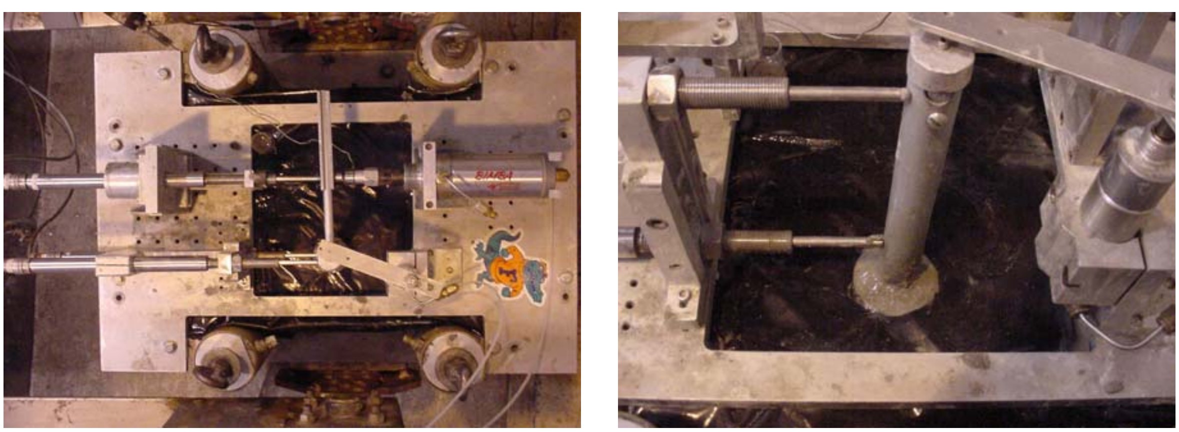

Figure 2.14 Model and the Shaft in the Soil

equivalent to 45 g while the shaft's cement was still fluid to equilibrate the soil and cement stresses to prototype values. A constant 45 g's of acceleration was maintained for 5 hours so that the cement grout would hydrate and reach a strength of 1000 psi upon which the lateral load test would commence.

2.4 Load Testing

After hydration of the cement (5 hours), the lateral load testing began. To prepare for testing, air pressure was applied to the small piston (Fig 2.14) attached to the top of structure, lifting it off the model. Next, the air pressure was switched to the big piston (Fig. 2.1) which applied load to the pole or mast arm. Throughout load phase, force (load cell, Fig 2.1) and displacements (LVDTs, Fig 2.1) were recorded using LabVIEW. As with the prior research (FDOT project: BC354, RPWO #9) the same failure criteria were employed. Specifically, lateral deflection of 12 inches or excessive rotation of 15° for g the foundation. A discussion of the tests performed and associated analysis is presented in Chapter Three.

CHAPTER 3
CENTRIFUGE TEST RESULTS

3.1 Test Plan

Presented in Table 3.1 is the centrifuge experiments performed with polymer (KB) slurries. The experiments involved a total of 16 tests, 8 with varied depth, loading, and soil conditions, and 2 for repetition. Evident from the table, the tests considered two different embedment depths (25′ & 35′), two different saturated sand states (loose and dense) and two different loading locations (mid mast and arm tip).

Table 3.1 Centrifuge Test Sequence (Polymer Slurry)

Test No.	Prototype Foundation Diameter (ft)	Type of Slurry	Prototype Embedment Length (ft)	Location of Applied Load		Soil State
				On Mid Mast Arm	On Tip of Mast Arm	
1	5	Polymer	25	*		Loose
2	5	Polymer	25		*	Loose
3	5	Polymer	25	*		Dense
4	5	Polymer	25		*	Dense
5	5	Polymer	35	*		Loose
6	5	Polymer	35		*	Loose
7	5	Polymer	35	*		Dense
8	5	Polymer	35		*	Dense

Note: The dry unit weight of loose sand is about 92.8 pcf (120.5 pcf in total unit weight).
The dry unit weight of dense sand is about 99.2 pcf (124.5 pcf in total unit weight).
Two more tests were performed for repeatability check.

3. 2 Torsional Resistance of Shafts Constructed with Polymer Slurry

As found in the earlier research (FDOT project: BC354, RPWO #9) with saturated sand deposits, failure occurred due to rotation (15°) at all embedments and loading (mid mast and arm tip), i.e., not with lateral deflections. The latter is attributed to the reduction in vertical and horizontal stresses in the soil along the shaft. Table 3.2 shows all of the measured prototype unit skin frictions at failure (15° rotation). The unit skin frictions were obtained by dividing the applied torque by the radius and the embedded shaft area. Evident from Table 3.2, measured unit skin friction of the drilled shaft in the dense sand was higher than the loose sand response.

Also given in Table 3.2 is the predicted unit skin friction using the axial skin friction model of O'Neill and implemented in The MathCAD program developed for high mast/sign design system (FDOT project: BC354, RPWO #9). Note the measured is higher for the shorter shafts than predicted. One possible explanation is the predicted model does not consider tip resistance (no cleanout specified).

Different from the mineral slurry results is the higher skin friction for the dense sand compared to the loose sand. For instance, consider the mid mast results, dense sand was 34% and 27% higher than the predicted response versus 14% and 8% for the loose sand. O'Neill and Majano documented the phenomenon that the torsional capacity of the sand increases with the use of polymer slurry in a three and a half year study for the United States Federal Highways Administration and ADSC (1993).

From the latter study, a shear strength increase of 50% was found for polymer slurries used in dense sand. Ata and O'Neill (2000) performed microscopic examination of the sand samples subject to polymer slurries at small pressure heads. The study revealed that polymer strands were present in the narrow pores of different diameters and shapes, and at variable distance from the slurry source. Moreover, the strands acted as soil reinforced in the soil formation (Ata, and O'Neill, M., 2000), similar to the cohesion in the clay. This could be one possible explanation for the increase of the torsional capacity.

Table 3. 2 Results of Combined Torsional and Lateral Centrifuge Tests Using KB Polymer Slurry

Point of Load Application	Relative Density (%)	Length to Diameter Ratio	Applied Torque (ft-kips)	Measured Shear Strength (psi)	Failure Mode	Measured Average Shear Strength (psi)	Predicted Shear Strength (psi)	Ratio (Measured Shear Strength to Predicted Shear Strength)	Errors (Difference between Measured and Predicted) (%)
Mid Mast Arm	69	5	1785	9.91	Torsional-Lateral	9.91	5.46	1.82	45%
	34		1082	5.93	Torsional-Lateral	5.93	5.11	1.16	14%
Arm Tip	69	5	1493	8.40	Torsional	8.40	5.46	1.54	35%
	34		1145	6.57	Torsional	6.57	5.11	1.29	22%
Mid Mast Arm	69	7	2417	9.81	Torsional	10.16	6.74	1.51	34%
	69		2284	10.50					
	34		1565	7.31	Torsional-Lateral	7.31	6.31	1.16	14%
Arm Tip	69	7	2032	9.21	Torsional	9.21	6.74	1.37	27%
	34		1512	6.85	Torsional	6.88	6.31	1.09	8%
	34		1526	6.91					

The sand used for research before was fine or medium dense sand, and there is very little literature about the effect of polymer slurry on loose sand. Based on the centrifuge tests result, the effect of polymer slurry was very limited for loose sand. A possible reason is that the pores in loose sand are larger and better connected compared to dense sand. Consequently, it is more difficult to form stable polymer strands in the pores of loose sand.

3. 3 Reduction of Lateral Capacity due to Torsional Loading

From previous dry as well as saturated sand tests (FDOT project: BC354, RPWO #9), it was concluded that there was a reduction in lateral capacity of a drilled shaft when subject to combined lateral and torsional loading. The magnitude of the reduction depends on the ratio of the torque to lateral load (eccentricity of the lateral load), and the length to diameter ratio of the drilled shaft. Figure 3.1 shows the reduction of lateral capacity due to a load applied at any point along the mast arm reported by the previous research (FDOT project: BC354, RPWO #9). Shown in Figure 3.2 is the measured and predicted load vs. deflected response for shafts under different torque to lateral load ratio constructed with bentonite slurry. Multiplying the lateral load test results with reduction factors, which were obtained from Fig 3.1, generated the two prediction lines. It was very apparent that the lateral capacity had significant reductions with the applied torque. Generally in the earlier study it was found that most of the measured results had slightly higher capacity than the predicted response, i.e., conservative. An exception was the 25-ft embedment, dense sand case, which had exactly the same measured and predicted response. Also, the earlier study (FDOT project: BC354, RPWO #9) determined that the same reduction factors should be used for both dry sand and saturated sand.

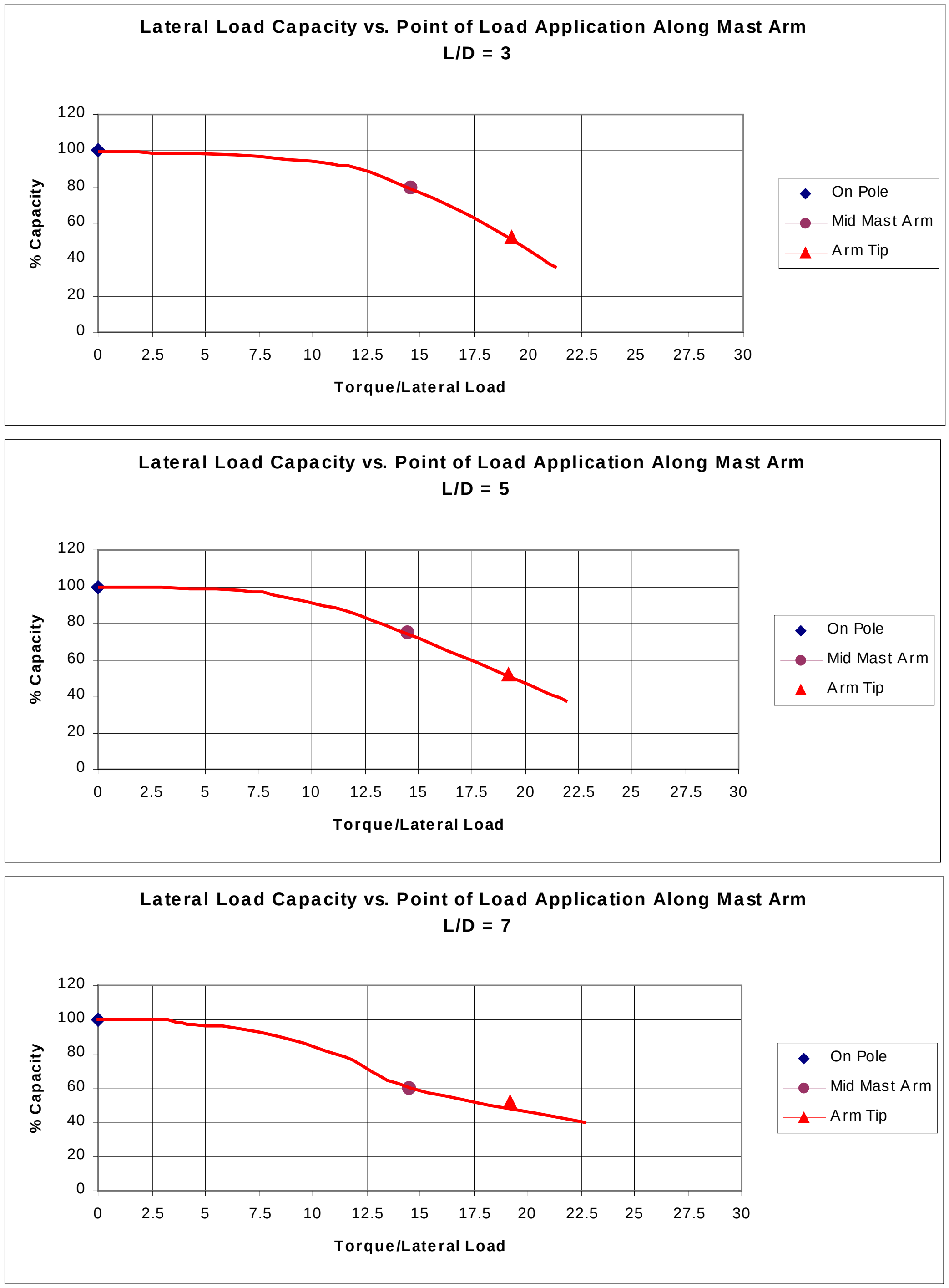

Figure 3.1 Reduction of Lateral Capacity as a Function of Torque to Lateral Load Ratio

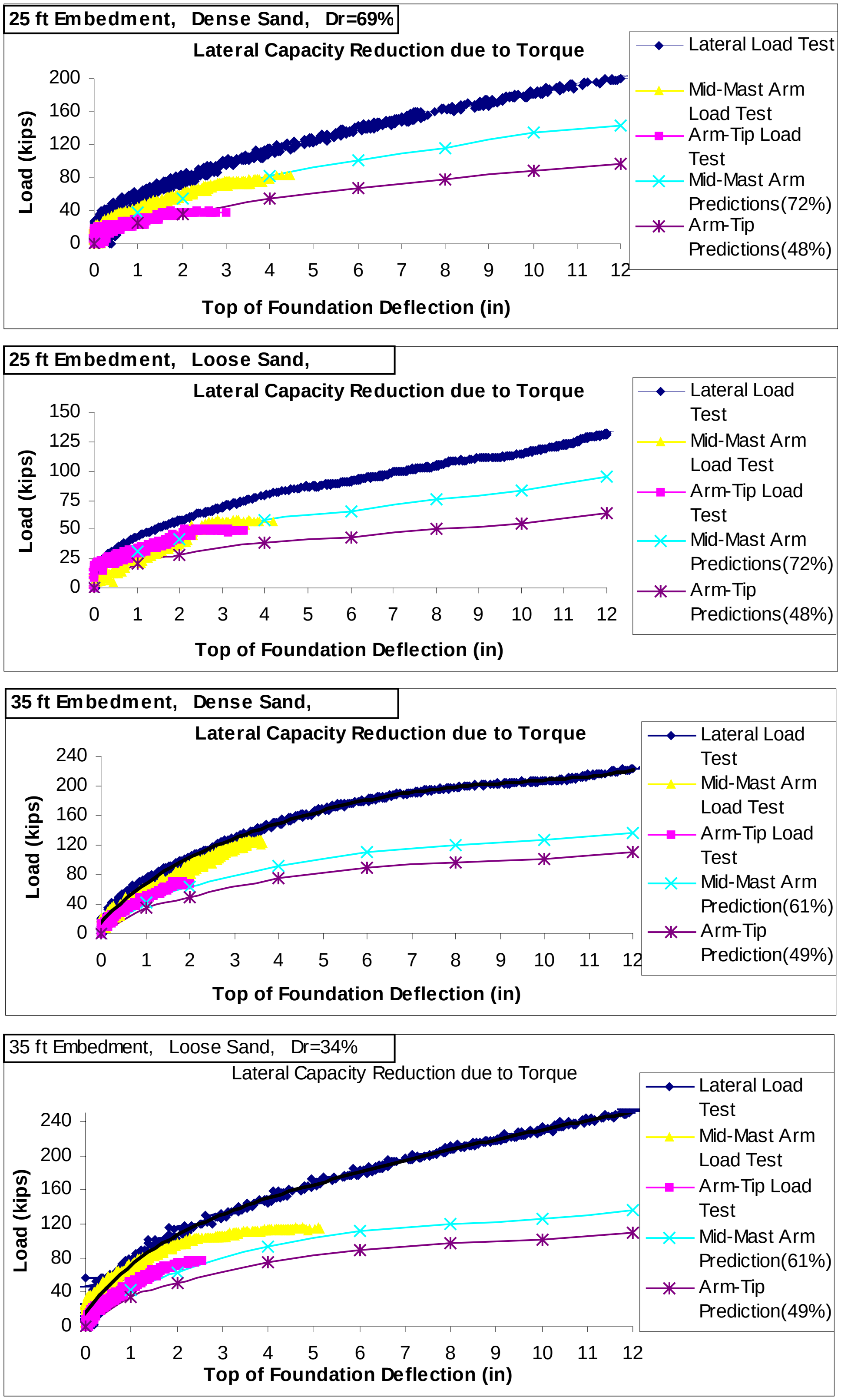

Figure 3. 2 Lateral Loads vs. Deformation for Saturated Sand with Bentonite Slurry

Figure 3.3 shows the measured response for shafts constructed in saturated sand using polymer slurry. In the case of the predicted response (mid mast & arm tip), the lateral reduction as suggested by Figure 3.1 was used. A comparison of measured and predicted shows in general that the predicted response is slightly conservative. As with the torsional resistance, the dense sands is exhibiting higher lateral capacities compared to the loose sand constructed with polymer slurry from the polymer strand reinforcement, which is occurring for dense sand and not for the loose sand.

A comparison of the bentonite and polymer slurry results is presented in Figure 3.4. Evident from the figure, the ultimate lateral capacities of the bentonite and polymer slurry tests are comparable for the loose sands, but for dense sand tests, the ultimate lateral capacities of the dense sands in polymer slurries are higher than the bentonite results. The latter is especially true for dense sands with arm tip loading, which has the highest torsional shear loading.

Since sand density may vary with depth, and FDOT does not distinguish between polymer and bentonite slurry construction, it was decided to employ the same lateral reduction curve (Figure 3.1) for all drilled shafts techniques (case, mineral and polymer slurry) subject to torque (conservative). It should be noted that significant head loss occurs under polymer slurry construction. Consequently, if slurry head is not maintained in the hole, then wall softening, and even collapse is possible which would negate any increased torsional resistance of a shaft (i.e., dense sands) due to polymer reinforcement. All of the centrifuge results (raw data) can be found in the Appendix A.

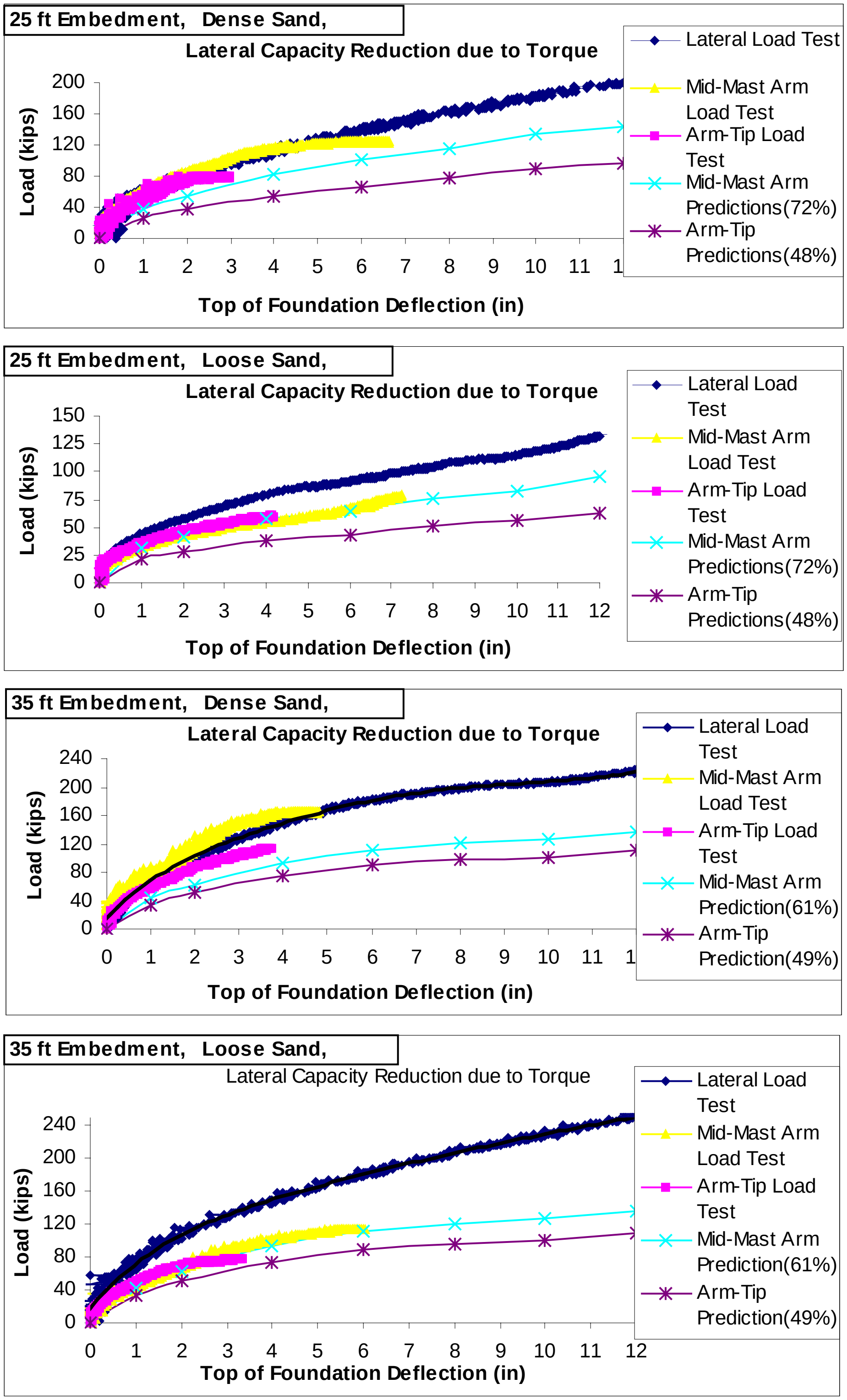

Figure 3. 3 Lateral Loads vs. Deflection in Saturated Sand with KB Polymer Slurry

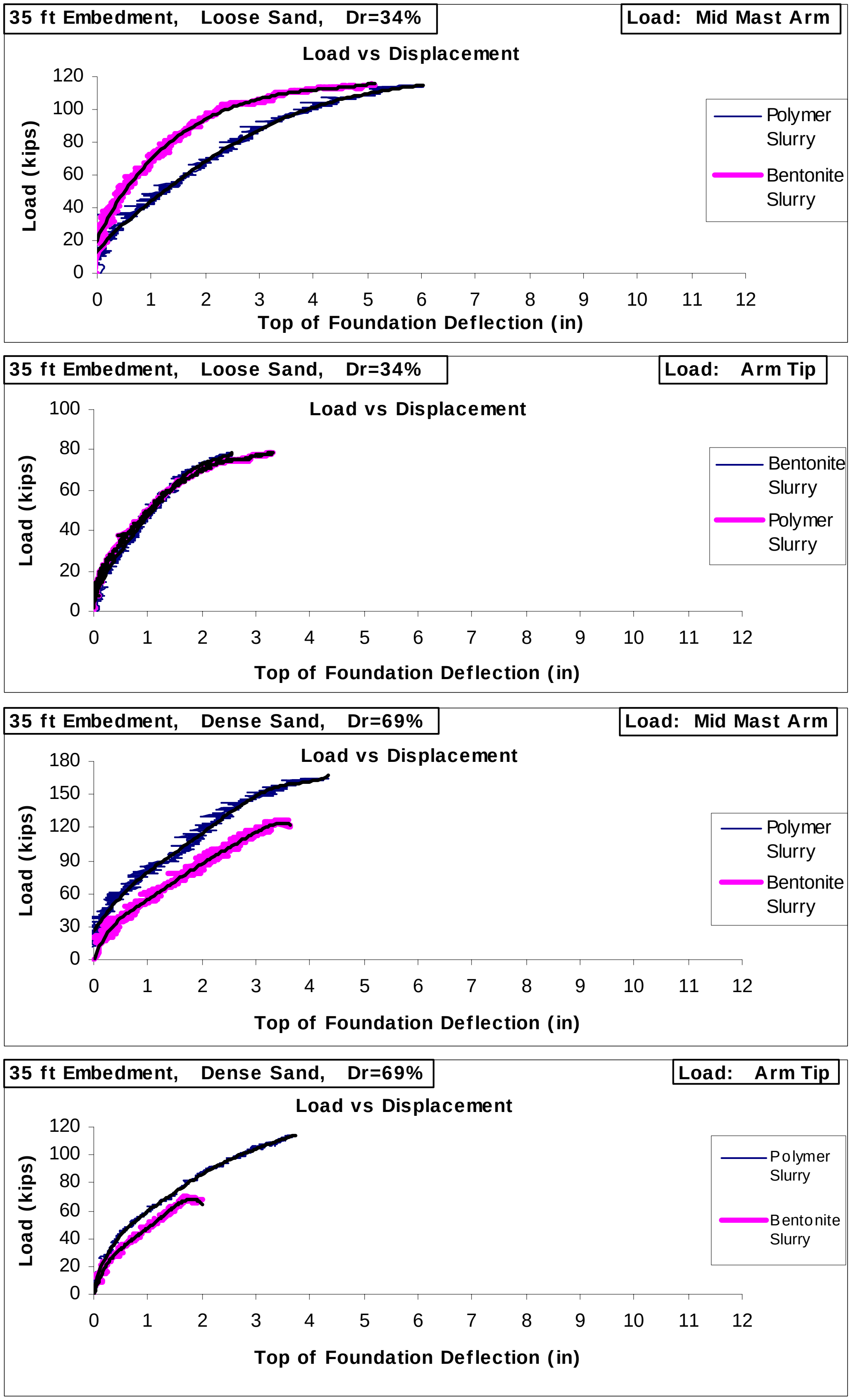

Figure 3.4 Comparison between Polymer Slurry Tests and Bentonite Slurry Tests

CHAPTER 4
CONCLUSIONS AND RECOMMENDATIONS

4.1 Conclusions

A series of centrifuge tests were performed on high mast signs supported on drilled shafts subject to lateral and torsional loading. The tests, involved construction of drilled shaft in saturated loose and dense sands involving polymer slurry. The study included two sand densities, three different load application points (i.e., torque to lateral load ratio), and two different embedment lengths.

Based on the measured centrifuge results, the following conclusions are drawn:

1. For both loose and dense saturated sands, the shafts failed by torsion. The failure is attributed to the significant reduction in effective stress (approximately ½); for sands, a reduction by 50% in the vertical and horizontal effective stress will reduce the torsional resistance by a similar amount (i.e., 50%).
2. The use of polymer slurry in construction of the drilled shaft did not reduce the shaft's torsional capacity like the possibility with bentonite slurry. Moreover, it was found that polymer slurry did not form a cake at the borehole wall, no matter how long the slurry was in the hole or how thick the polymer became. In addition, for some cases (i.e., dense sand tests), the torsional capacity of the shaft increased (the maximum increase is 45%). The latter was attributed polymer slurry reinforcement in the sand which gave it cohesion like tendencies (Atta and O'Neill, 2000).
3. The reduction in lateral capacity due to torque was observable/measurable from the onset of loading and is a function of Torque to Lateral Load ratio and L/D ratio as reported in earlier research (Fig. 3.1 and FDOT project: BC354, RPWO #9).

4. Prediction of measured response with the MathCAD developed software (FDOT project: BC354, RPWO #9) gave satisfactory predictions for both the lateral and torsional capacity of the drilled shafts in saturated sand. It also indicated the appropriate shaft failure (i.e., lateral or torsion). The new design version will select both the diameter and shaft length for given load, eccentricity, and safety factor based on combined lateral and torsional analysis. The user also has an option of selecting a diameter, and the program can determine shaft length if the diameter meets the lateral requirements.

4.2 Recommendations

The following are some suggestions on future research as an outcome of this work:

1. The polymer slurry was found to increase the torsional capacity of drilled shafts. Of interest is the understanding why it occurs to a greater extent in dense sand than loose sand.
2. The reduction of lateral capacity due to torque in cohesionless soil has been completed along with proposed guidelines. It is suggested that similar study be undertaken for cohesive soil, along with new guidelines if needed.
3. It is proposed that the reduction in lateral resistance due to torque may be explained from the failure wedge approach of Reese (1973) with the inclusion of torsional shear stress. However, numerical FEM analysis should be undertaken to identify the shape of the failure wedge around the shaft with both lateral and torsional stresses.

REFERENCES

Ata, A., and O'Neill, M., "Physiochemical Interaction Between PHPA Polymer Slurry and Cement Mortar," *ASTM Geotechnical Testing Journal*, GTJODJ, Vol. 23, No. 1, June 2000, pp. 231-241.

Bradley, D., *Centrifugal Scaling Laws for Ground Launch Cruise Missile Shelter, Final Report*, Air Force Engineering and Services Center, Tyndall, AFB, Florida, No. ESL-TR-84-07, April 1984.

Majano. R., and O'Neill, M., "Effects of Mineral and Polymer Slurries on Perimeter Load Transfer in Drilled Shafts," *Report to ADSC, International Association of Foundation Drilling*, January 1993, 336 p.

McVay, M.C., Herrera, R., and Hu, Z., "Determine Optimum Depths of Drilled Shafts Subject to Combined Torsion and Lateral Loads Using Centrifuge Testing," *Final Report* to Florida Department of Transportation, Contract: BC354, RPWO #9, April 2003, 189 p.

Reese, L.C., Cox, W.R., and Koop, F.D., "Analysis of Laterally Loaded Piles in Sand," *Proceedings, Sixth Annual Offshore Technology Conference*, Vol. 2, Houston Texas, May 1973, pp. 246-258.

Reese, L.C., and O'Neill, M., *Drilled Shafts Student Workbook*, FHWA, FHWA-HI-88-042, U.S. Department of Transportation, 1988.

APPENDIX A

CENTRIFUGE TEST RESULTS
(KB POLYMER SLURRY)

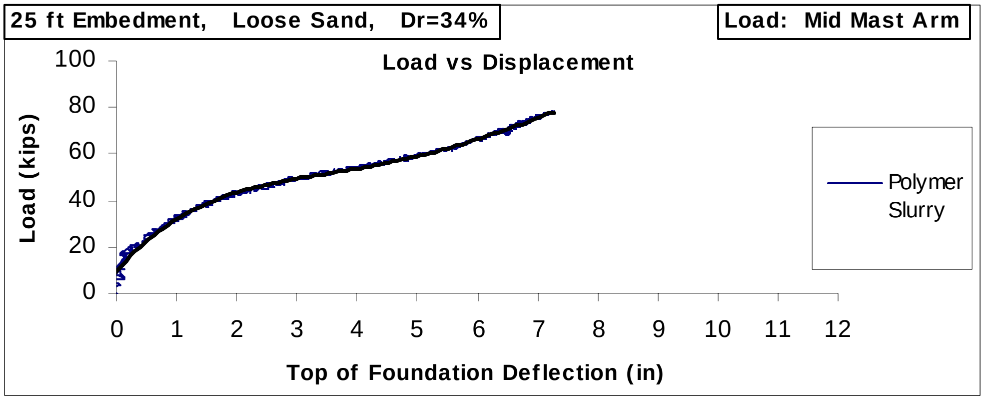
25 ft Embedment, Loose Sand, Dr=34%
Load: Mid Mast Arm
Load vs Displacement
Load (kips)
Top of Foundation Deflection (in)
Polymer Slurry

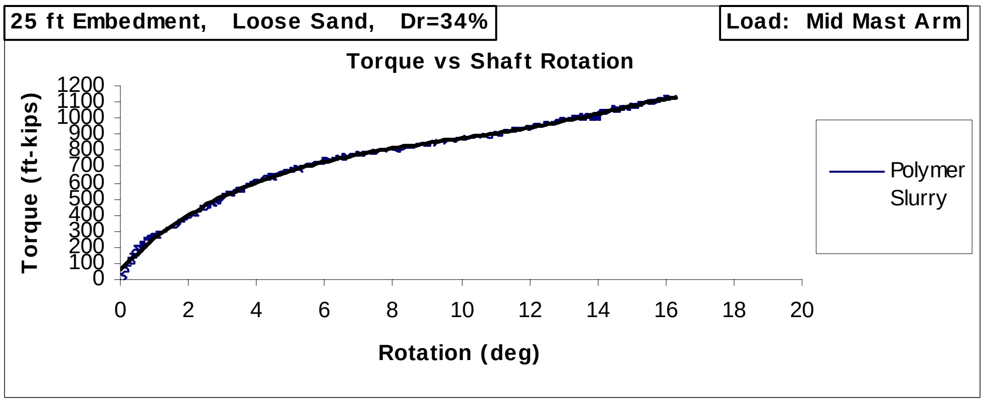
25 ft Embedment, Loose Sand, Dr=34%
Load: Mid Mast Arm
Torque vs Shaft Rotation
Torque (ft-kips)
Rotation (deg)
Polymer Slurry

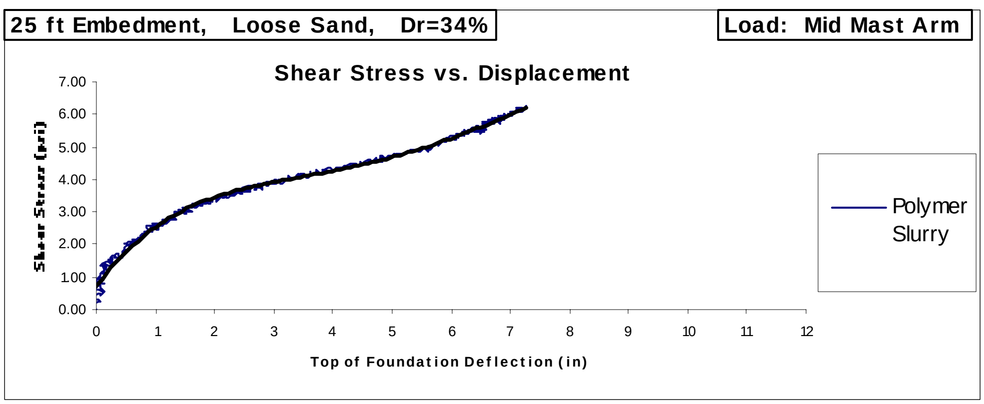
25 ft Embedment, Loose Sand, Dr=34%
Load: Mid Mast Arm
Shear Stress vs. Displacement
Shear Stress (psi)
Top of Foundation Deflection (in)
Polymer Slurry

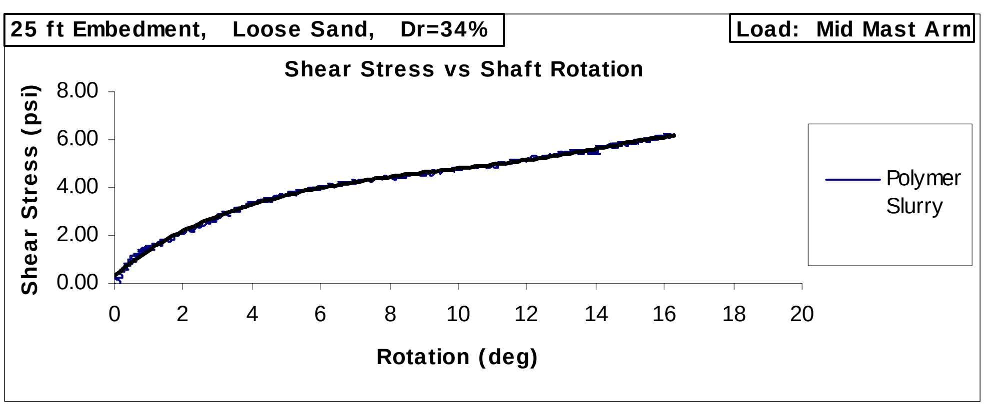
25 ft Embedment, Loose Sand, Dr=34%
Load: Mid Mast Arm
Shear Stress vs Shaft Rotation
Shear Stress (psi)
Rotation (deg)
Polymer Slurry

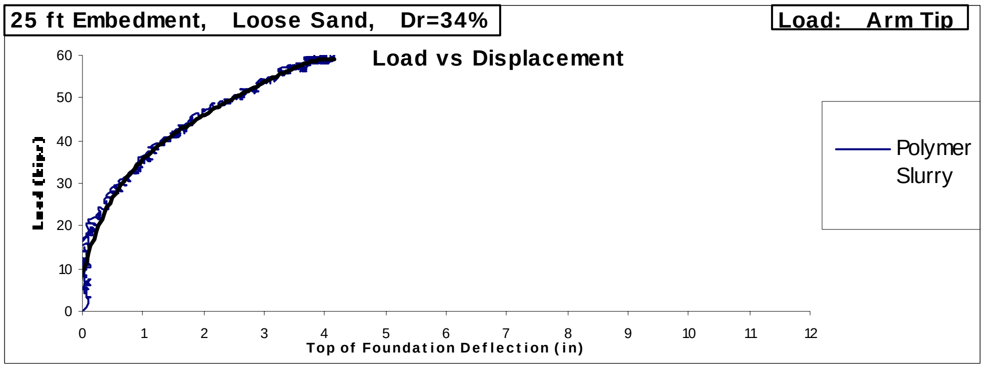
25 ft Embedment, Loose Sand, Dr=34%
Load: Arm Tip
Load vs Displacement
Top of Foundation Deflection (in)
Polymer Slurry

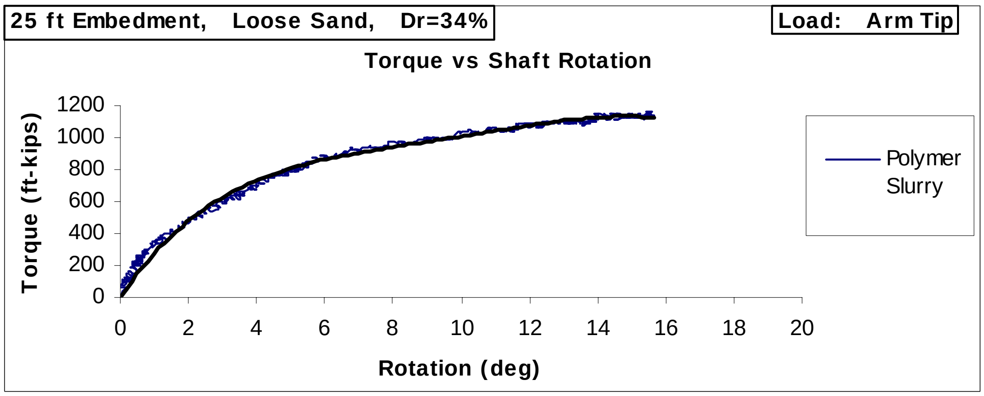
25 ft Embedment, Loose Sand, Dr=34%
Load: Arm Tip
Torque vs Shaft Rotation
Torque (ft-kips)
Rotation (deg)
Polymer Slurry

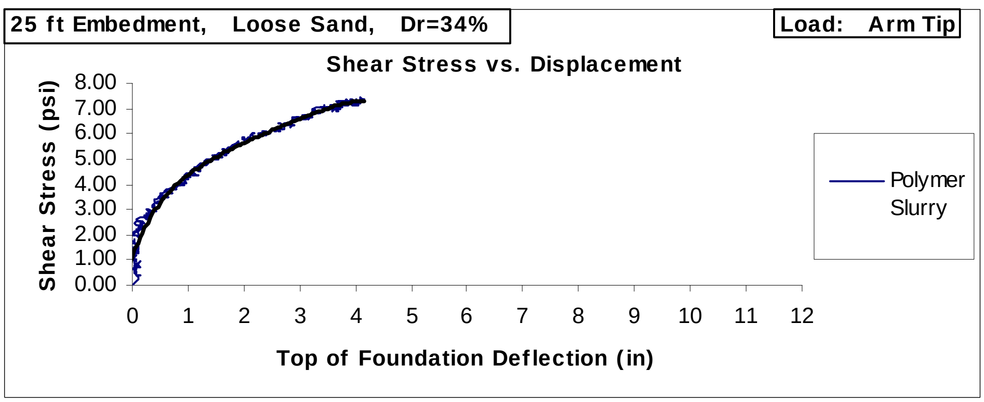
25 ft Embedment, Loose Sand, Dr=34%
Load: Arm Tip
Shear Stress vs. Displacement
Shear Stress (psi)
Top of Foundation Deflection (in)
Polymer Slurry

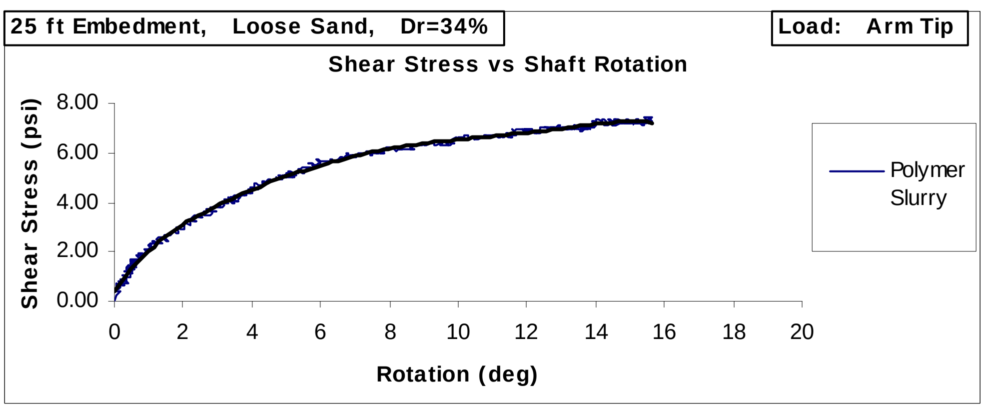
25 ft Embedment, Loose Sand, Dr=34%
Load: Arm Tip
Shear Stress vs Shaft Rotation
Shear Stress (psi)
Rotation (deg)
Polymer Slurry

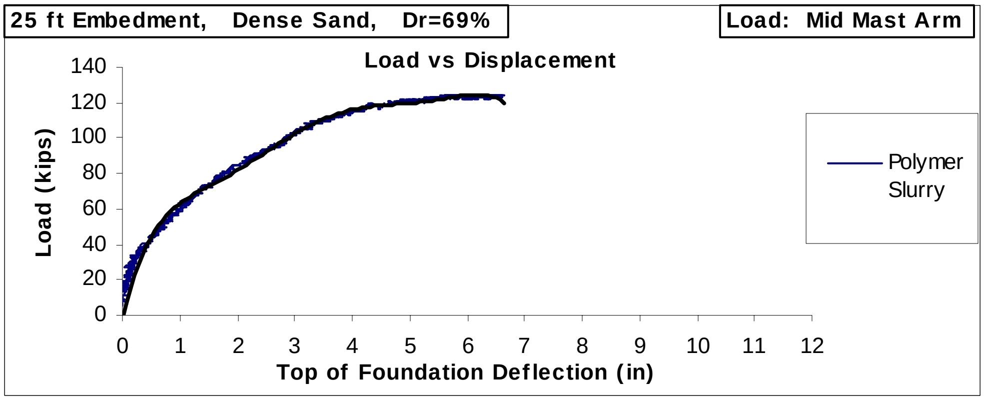
25 ft Embedment, Dense Sand, Dr=69%
Load: Mid Mast Arm
Load vs Displacement
Load (kips)
Top of Foundation Deflection (in)
Polymer Slurry

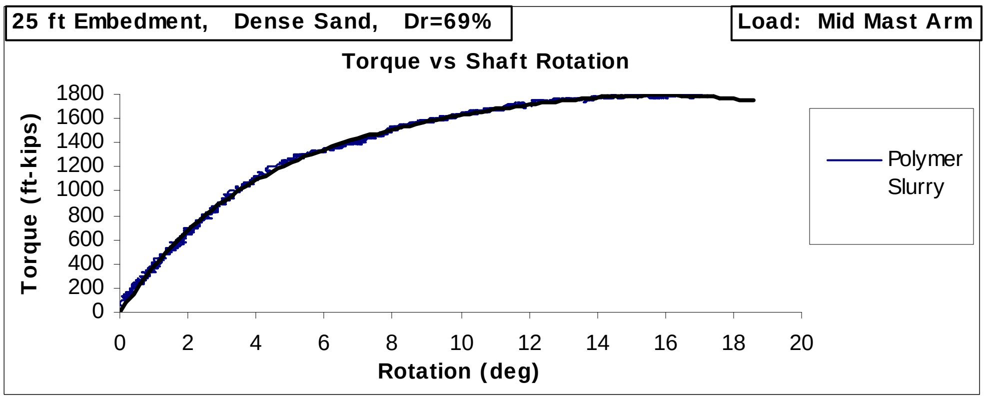
25 ft Embedment, Dense Sand, Dr=69%
Load: Mid Mast Arm
Torque vs Shaft Rotation
Torque (ft-kips)
Rotation (deg)
Polymer Slurry

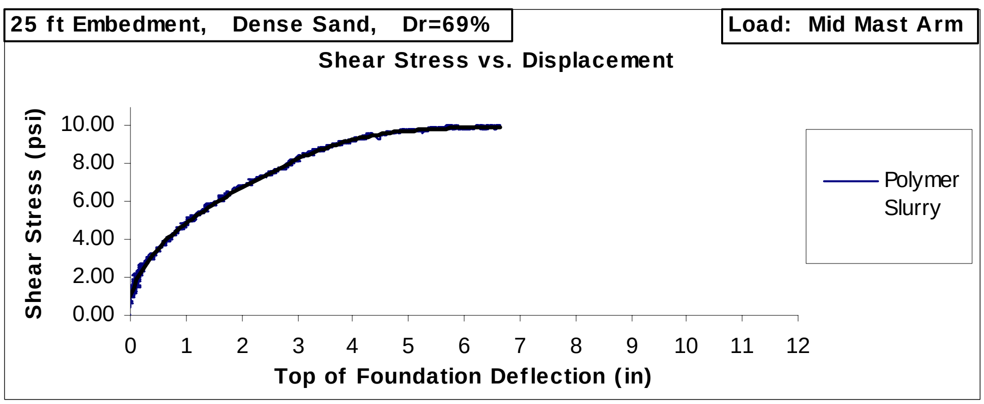
25 ft Embedment, Dense Sand, Dr=69%
Load: Mid Mast Arm
Shear Stress vs. Displacement
Shear Stress (psi)
Top of Foundation Deflection (in)
Polymer Slurry

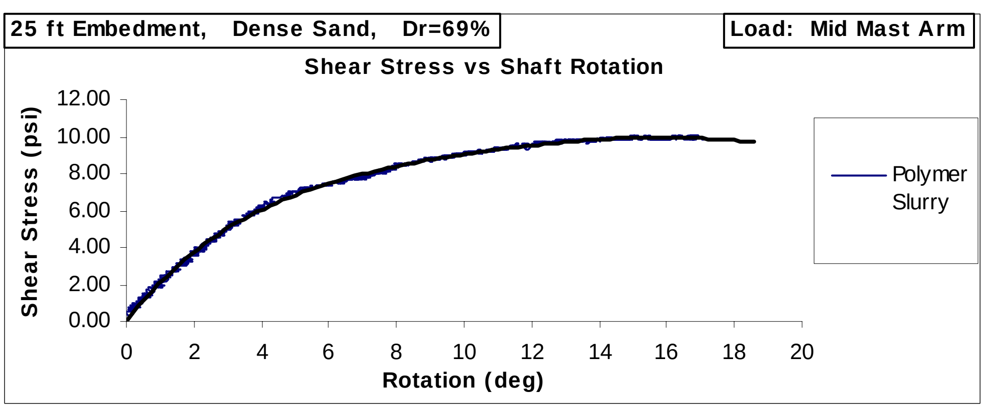
25 ft Embedment, Dense Sand, Dr=69%
Load: Mid Mast Arm
Shear Stress vs Shaft Rotation
Shear Stress (psi)
Rotation (deg)
Polymer Slurry

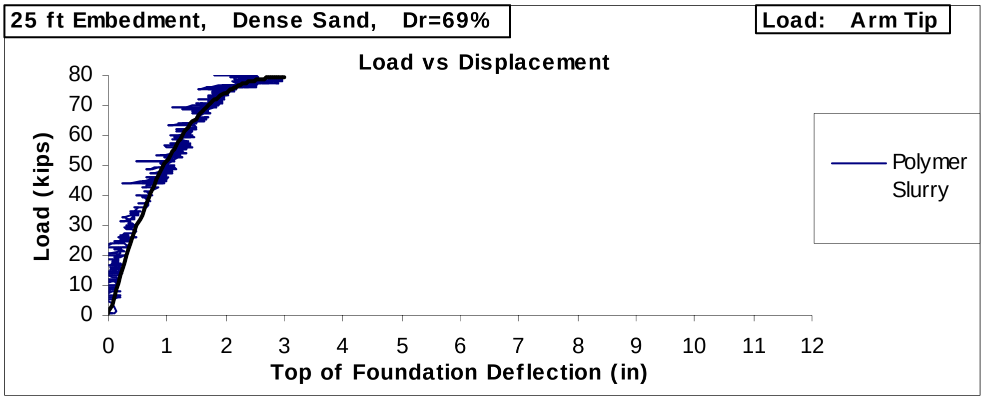
25 ft Embedment, Dense Sand, Dr=69%
Load: Arm Tip
Load vs Displacement
Load (kips)
80
70
60
50
40
30
20
10
0
0 1 2 3 4 5 6 7 8 9 10 11 12
Top of Foundation Deflection (in)
Polymer Slurry

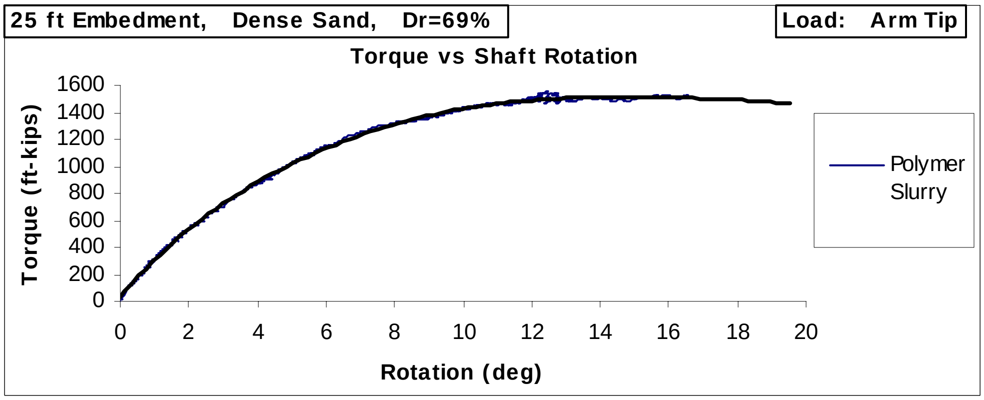
25 ft Embedment, Dense Sand, Dr=69%
Load: Arm Tip
Torque vs Shaft Rotation
Torque (ft-kips)
1600
1400
1200
1000
800
600
400
200
0
0 2 4 6 8 10 12 14 16 18 20
Rotation (deg)
Polymer Slurry

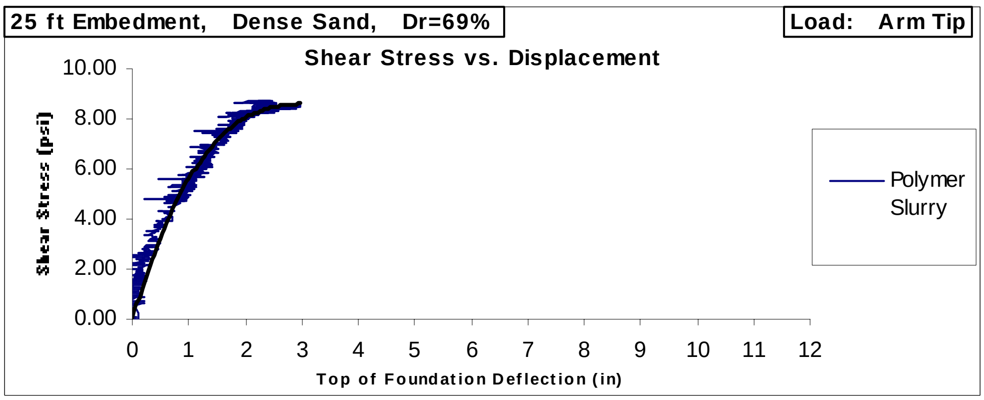
25 ft Embedment, Dense Sand, Dr=69%
Load: Arm Tip
Shear Stress vs. Displacement
Shear Stress (psi)
10.00
8.00
6.00
4.00
2.00
0.00
0 1 2 3 4 5 6 7 8 9 10 11 12
Top of Foundation Deflection (in)
Polymer Slurry

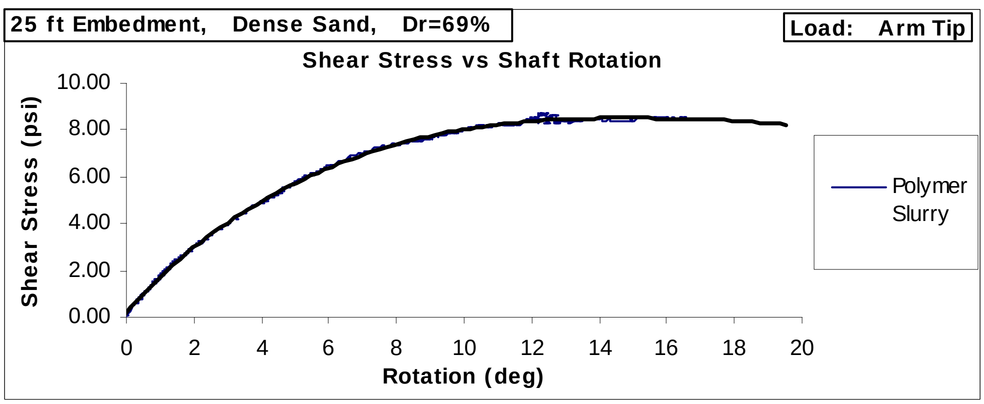
25 ft Embedment, Dense Sand, Dr=69%
Load: Arm Tip
Shear Stress vs Shaft Rotation
Shear Stress (psi)
10.00
8.00
6.00
4.00
2.00
0.00
0 2 4 6 8 10 12 14 16 18 20
Rotation (deg)
Polymer Slurry

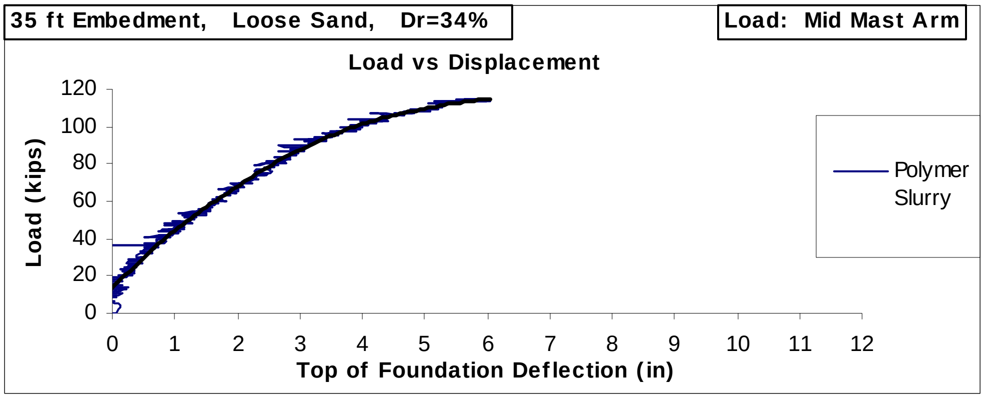
35 ft Embedment, Loose Sand, Dr=34%
Load: Mid Mast Arm
Load vs Displacement
Load (kips)
0
20
40
60
80
100
120
0
1
2
3
4
5
6
7
8
9
10
11
12
Top of Foundation Deflection (in)
Polymer Slurry

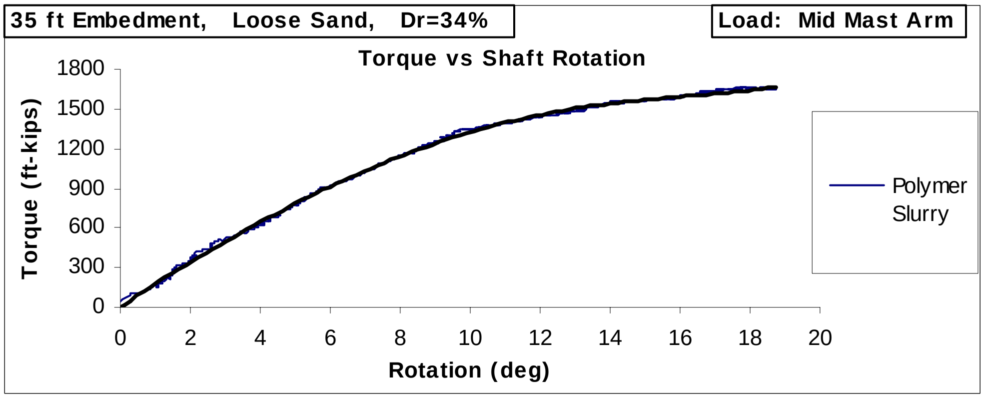
35 ft Embedment, Loose Sand, Dr=34%
Load: Mid Mast Arm
Torque vs Shaft Rotation
Torque (ft-kips)
0
300
600
900
1200
1500
1800
0
2
4
6
8
10
12
14
16
18
20
Rotation (deg)
Polymer Slurry

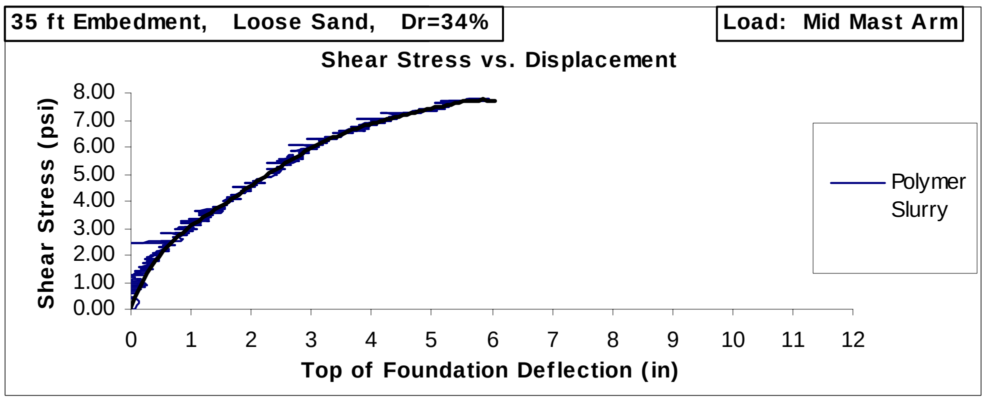
35 ft Embedment, Loose Sand, Dr=34%
Load: Mid Mast Arm
Shear Stress vs. Displacement
Shear Stress (psi)
0.00
1.00
2.00
3.00
4.00
5.00
6.00
7.00
8.00
0
1
2
3
4
5
6
7
8
9
10
11
12
Top of Foundation Deflection (in)
Polymer Slurry

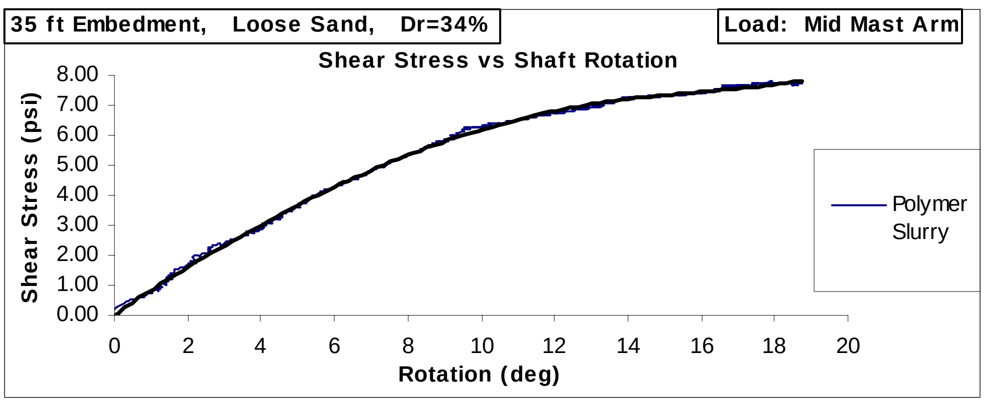
35 ft Embedment, Loose Sand, Dr=34%
Load: Mid Mast Arm
Shear Stress vs Shaft Rotation
Shear Stress (psi)
0.00
1.00
2.00
3.00
4.00
5.00
6.00
7.00
8.00
0
2
4
6
8
10
12
14
16
18
20
Rotation (deg)
Polymer Slurry

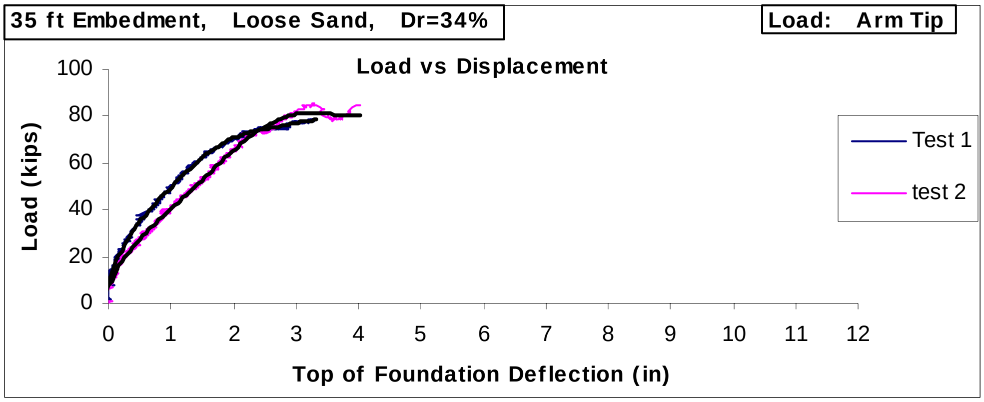
35 ft Embedment, Loose Sand, Dr=34%
Load: Arm Tip
Load vs Displacement
Load (kips)
100
80
60
40
20
0
0 1 2 3 4 5 6 7 8 9 10 11 12
Top of Foundation Deflection (in)
Test 1
test 2

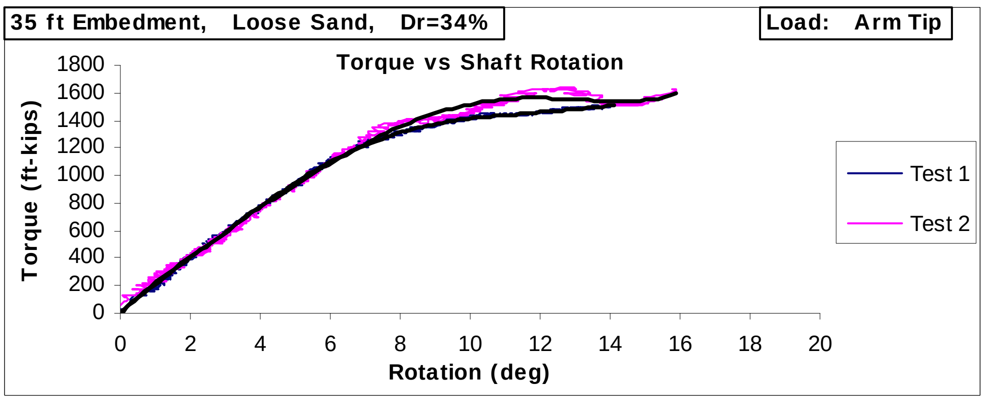
35 ft Embedment, Loose Sand, Dr=34%
Load: Arm Tip
Torque vs Shaft Rotation
Torque (ft-kips)
1800
1600
1400
1200
1000
800
600
400
200
0
0 2 4 6 8 10 12 14 16 18 20
Rotation (deg)
Test 1
Test 2

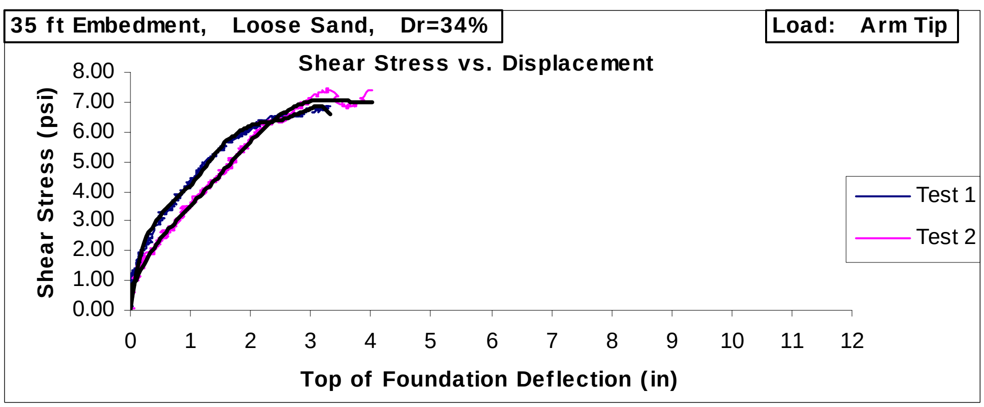
35 ft Embedment, Loose Sand, Dr=34%
Load: Arm Tip
Shear Stress vs. Displacement
Shear Stress (psi)
8.00
7.00
6.00
5.00
4.00
3.00
2.00
1.00
0.00
0 1 2 3 4 5 6 7 8 9 10 11 12
Top of Foundation Deflection (in)
Test 1
Test 2

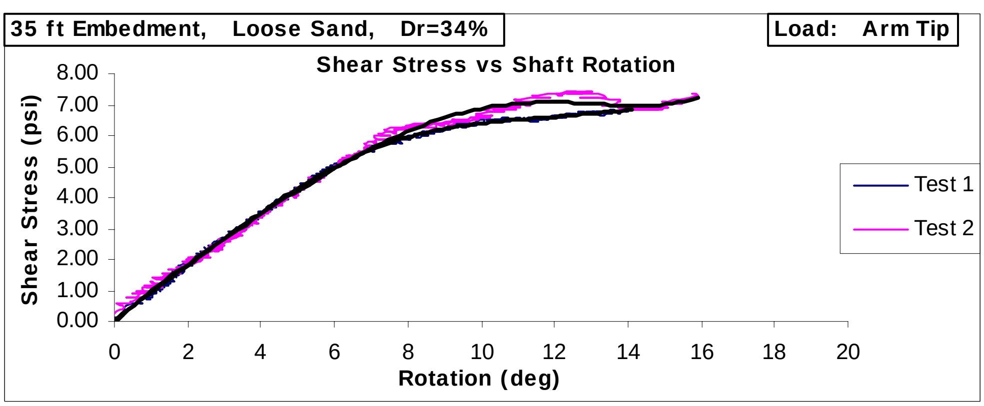
35 ft Embedment, Loose Sand, Dr=34%
Load: Arm Tip
Shear Stress vs Shaft Rotation
Shear Stress (psi)
8.00
7.00
6.00
5.00
4.00
3.00
2.00
1.00
0.00
0 2 4 6 8 10 12 14 16 18 20
Rotation (deg)
Test 1
Test 2

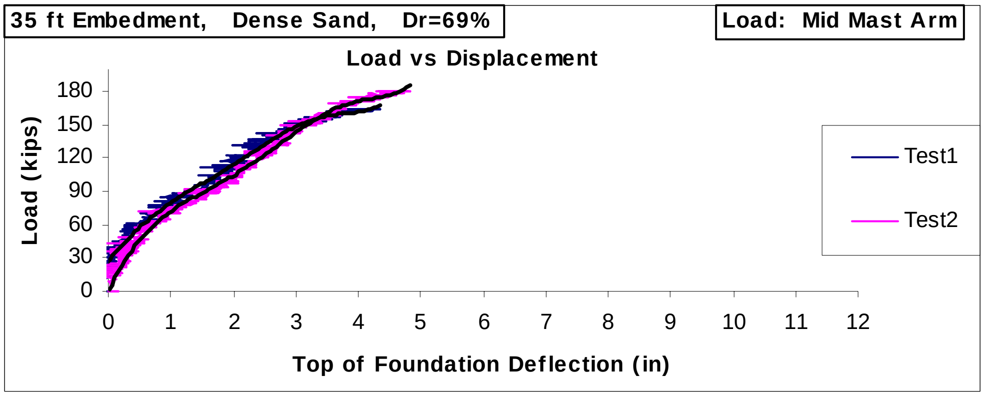
35 ft Embedment, Dense Sand, Dr=69%
Load: Mid Mast Arm
Load vs Displacement
Load (kips)
180
150
120
90
60
30
0
0 1 2 3 4 5 6 7 8 9 10 11 12
Top of Foundation Deflection (in)
Test1
Test2

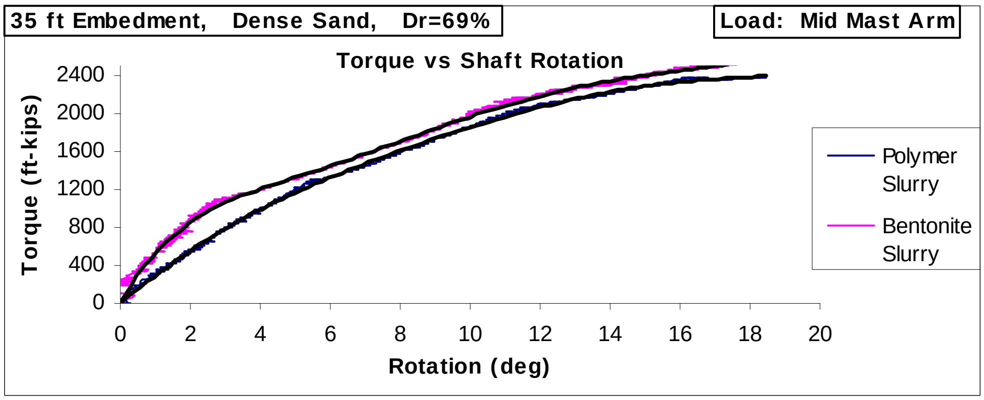
35 ft Embedment, Dense Sand, Dr=69%
Load: Mid Mast Arm
Torque vs Shaft Rotation
Torque (ft-kips)
2400
2000
1600
1200
800
400
0
0 2 4 6 8 10 12 14 16 18 20
Rotation (deg)
Polymer Slurry
Bentonite Slurry

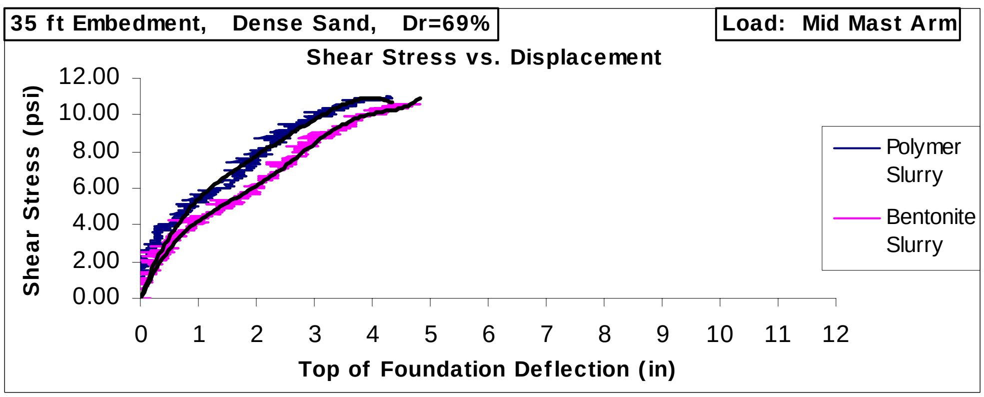
35 ft Embedment, Dense Sand, Dr=69%
Load: Mid Mast Arm
Shear Stress vs. Displacement
Shear Stress (psi)
12.00
10.00
8.00
6.00
4.00
2.00
0.00
0 1 2 3 4 5 6 7 8 9 10 11 12
Top of Foundation Deflection (in)
Polymer Slurry
Bentonite Slurry

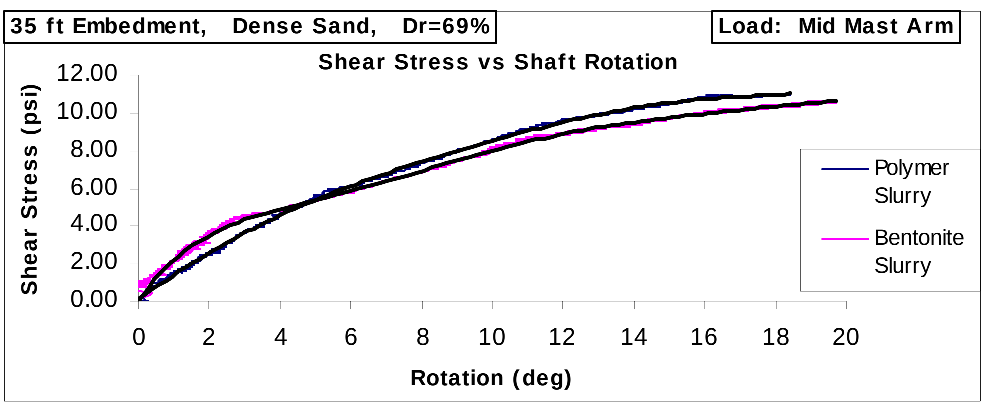
35 ft Embedment, Dense Sand, Dr=69%
Load: Mid Mast Arm
Shear Stress vs Shaft Rotation
Shear Stress (psi)
12.00
10.00
8.00
6.00
4.00
2.00
0.00
0 2 4 6 8 10 12 14 16 18 20
Rotation (deg)
Polymer Slurry
Bentonite Slurry

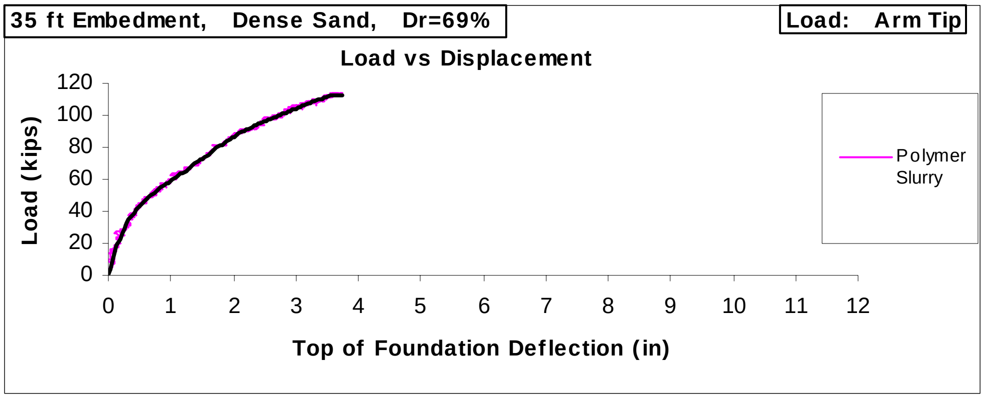
35 ft Embedment, Dense Sand, Dr=69%
Load: Arm Tip
Load vs Displacement
Load (kips)
120
100
80
60
40
20
0
0 1 2 3 4 5 6 7 8 9 10 11 12
Top of Foundation Deflection (in)
Polymer Slurry

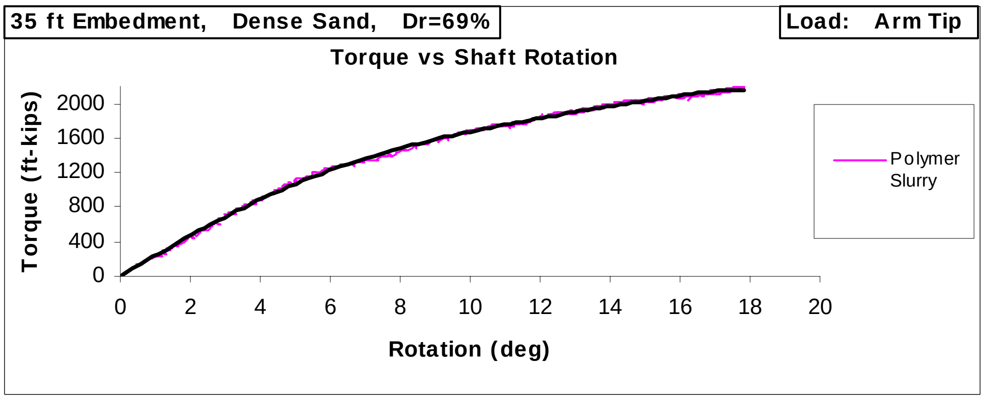
35 ft Embedment, Dense Sand, Dr=69%
Load: Arm Tip
Torque vs Shaft Rotation
Torque (ft-kips)
2000
1600
1200
800
400
0
0 2 4 6 8 10 12 14 16 18 20
Rotation (deg)
Polymer Slurry

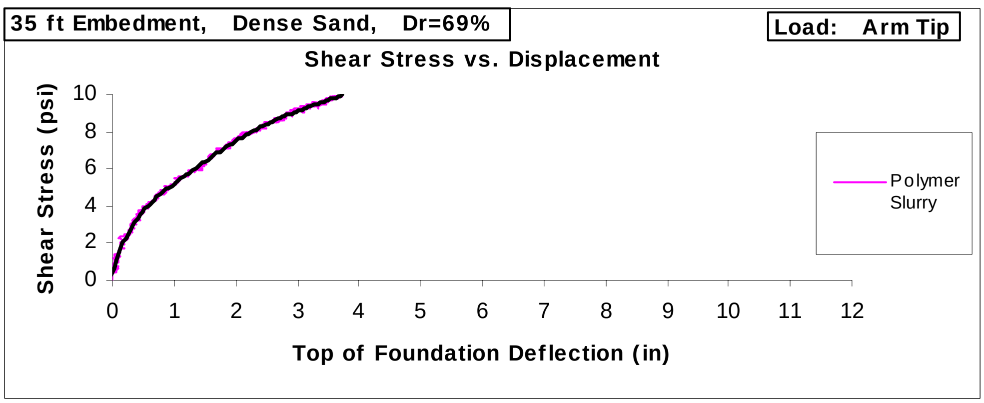
35 ft Embedment, Dense Sand, Dr=69%
Load: Arm Tip
Shear Stress vs. Displacement
Shear Stress (psi)
10
8
6
4
2
0
0 1 2 3 4 5 6 7 8 9 10 11 12
Top of Foundation Deflection (in)
Polymer Slurry

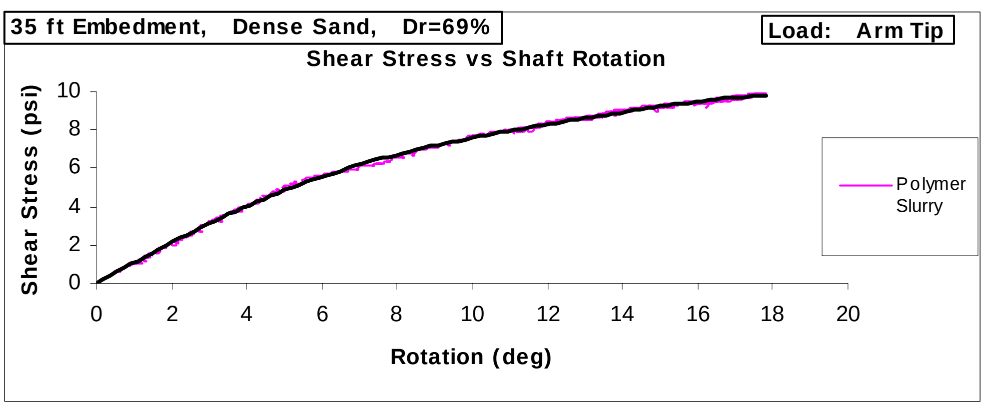
35 ft Embedment, Dense Sand, Dr=69%
Load: Arm Tip
Shear Stress vs Shaft Rotation
Shear Stress (psi)
10
8
6
4
2
0
0 2 4 6 8 10 12 14 16 18 20
Rotation (deg)
Polymer Slurry